



PERGAMON

Quaternary Science Reviews 0 (2001) 1-18



Flow variability in the Scandinavian ice sheet: modelling the coupling between ice sheet flow and hydrology

Neil Arnold^{a,*}, Martin Sharp^b

^a *Scott Polar Research Institute, University of Cambridge, Lensfield Road, Cambridge, CB2 1ER, UK*

^b *Department of Earth and Atmospheric Sciences, University of Alberta, Edmonton, AB, T6G 2E3, Canada*

Abstract

There is increasing geologic evidence for periodic flow variability within large ice sheets, manifested as spatially and temporally variable areas of fast ice flow, and resulting in the very complex patterns of lineations observed in formerly glaciated areas. However, many ice sheet models do not replicate this behaviour. A possible reason for this is that such models do not include a detailed treatment of basal hydrology. Changes in the character of sub-glacial drainage systems are believed to cause surges in valley glaciers. Recent ice sheet models, which have included basal hydrology or at least a link between basal velocity and the presence of water at the bed, often show flow variability. However, these models have typically assumed a deformable bed, or have made no assumptions about the nature of the bed. Whilst these assumptions seem applicable to areas close to the former margins of Quaternary ice sheets, they are less applicable to interior areas. These areas typically show thin or scanty till cover over eroded bedrock, and the presence of eskers, which are indicative of drainage in sub-glacial tunnels. We have developed a two-dimensional time-dependent ice sheet model that includes hard-bed basal hydrology. This allows calculation of sub-glacial water pressures and the use of a water pressure dependent sliding law to calculate ice sheet velocities. When used to simulate the Weichselian Scandinavian ice sheet, with late Quaternary climate and sea level as forcing functions, this model develops localised areas of fast-flowing ice, which vary in extent and in distance of penetration into the interior of the ice sheet both spatially and temporally. The behaviour of these lobes depends crucially on the influence of the evolving ice sheet topography on the routing of subglacial water flow, due to the resulting variations in the subglacial hydraulic potential which drive the water flow. Bedrock topography also has some influence, but fast flow areas are not confined to obvious topographic troughs. A relatively thin ice sheet with low surface slopes is produced in areas experiencing fast ice flow. Generally, two to four separate areas of fast flow can be recognised, and these are similar in size and shape to the 'lobes' identified in some geologically based reconstructions of the Scandinavian ice sheet. Within the fast-flowing areas, sub-glacial drainage is typically in a cavity-based system. However, tunnel-based drainage is predicted to have extended up to 150 km from the ice sheet margin, particularly during deglaciation. Because of the changes in ice sheet topography associated with fast flow, and the resulting changes in the pattern of sub-glacial water flow, the model predicts that these fast-flowing lobes interacted in complex ways, and exhibited quasi-periodic switching between fast and slow flow. © 2001 Published by Elsevier Science Ltd.

1. Introduction

There is increasing geologic evidence that large Quaternary ice sheets experienced periodic, internally driven oscillations. Such evidence includes so-called "Heinrich layers" in Atlantic marine sediments (Bond et al., 1992), and geomorphic evidence for localised fast flow within ice sheets. This is indicated by low gradient ice surface profiles (Mathews, 1974), localised long distance erratic transport and debris dispersal (Dyke and Morris, 1988), and "surge moraines" defining

former ice sheet margin positions (Dyke and Prest, 1987). In Scandinavia, Punkari (1984) described the episodic formation of up to 8 ice lobes during the last deglaciation and suggested that these consisted of 100–200 km wide areas of fast-flowing ice bordered by areas of more slowly moving ice.

Large-scale studies in both North America and Scandinavia, based on satellite imagery (e.g. Punkari, 1989; Boulton and Clark, 1990a, b; Clark, 1993; Boulton et al., 2001) or comprehensive compilations of geologic and geomorphic evidence (e.g. Kleman et al., 1997), also indicate a high degree of flow variability within large mid-latitude ice sheets during the Weichselian. The studies by Klemans et al. and Boulton et al. in particular make ambitious reconstructions of ice extent and

*Corresponding author. Tel.: +44-1223-336-540; fax: +44-1223-336-572.

E-mail address: nsa12@cus.cam.ac.uk (N. Arnold).

- 1 dynamics for the whole of the last glacial cycle. These 57
 2 studies conclude that the Scandinavian Ice Sheet 59
 3 exhibited complex patterns of flow variability during 59
 4 both glacial advance and retreat phases. Part of this 61
 5 complexity seemed to be due by the migration of the ice 61
 6 divide in response to climate change, but it also seemed 63
 7 to be due to the spatial and temporal variability of fast 63
 8 flowing areas of the ice sheet.
- 9 The high degree of flow variability implied by such 65
 10 studies is probably linked to changes in the nature of the 65
 11 bed of the ice sheet. Such changes could include a shift 67
 12 between frozen and thawed bed conditions, or a change 67
 13 in ambient water pressure conditions over a thawed bed. 69
 14 It could also include a switch between hard and soft bed 71
 15 conditions, although the occurrence of bed deformation 71
 16 is dependent not only upon the existence of sub-glacial 73
 17 sediment, but also upon the ambient water pressure. The 73
 18 occurrence of high water pressure is critical, as it allows 75
 19 rapid basal motion by sliding (Iken, 1981), deformation 75
 20 of weak sub-glacial sediments (Boulton and Hindmarsh, 77
 21 1987), or some combination of these processes (Iverson 77
 22 et al., 1995).
- 23 Many numerical ice sheet models have either 79
 24 neglected basal sliding or treated basal hydrology in 79
 25 only a simple way. As a result, they have not simulated 81
 26 spatially localised and temporally oscillatory fast flow 81
 27 (e.g. Huybrechts, 1992; Lindstrom, 1990). More re- 83
 28 cently, however, Payne (1995) found that a two- 83
 29 dimensional, thermomechanical flowline model, in 85
 30 which basal sliding was possible only where the bed of 85
 31 the ice sheet was at the pressure melting point, exhibited 87
 32 periodic oscillations. The area experiencing fast flow 87
 33 expanded headwards from the margin of the ice sheet, 89
 34 until the ice sheet thinned and flattened sufficiently that 89
 35 the bed re-froze and fast flow stopped. In a three- 91
 36 dimensional model, this instability was manifest as 91
 37 spatially discrete, but temporally stable, areas of fast 93
 38 flow, apparently analogous to ice streams (Payne and 93
 39 Dongelmans, 1997). In an application of this model to 95
 40 the West Antarctic Ice Sheet, Payne (1998, 1999) 95
 41 produced similar flow features. In this case, however, 97
 42 the Siple Coast ice streams (in particular Ice Streams A, 97
 43 B, and C) interacted with each other via an 'ice capture' 99
 44 mechanism, which resulted in quasi-periodic flow 99
 45 variability. In these studies, a melting bed is a sufficient 101
 46 condition for fast flow, and there is no treatment of the 101
 47 basal hydrological system. This is significant because it 103
 48 is widely believed that the configuration of the sub- 103
 49 glacial drainage system can exert considerable influence 105
 50 on basal motion through the effect of the sub-glacial 105
 51 water pressure on rates of sliding and/or bed deforma- 107
 52 tion (e.g. Iken, 1981; Kamb, 1987; Fowler, 1987a, b).
- 53 In a separate modelling development, Fowler and co- 109
 54 workers (Fowler and Johnson, 1995, 1996; Fowler and 109
 55 Schiavi, 1998) have produced a model to evaluate 111
 56 'surging' by ice sheets, in which a melting bed is only 111
- a necessary condition that allows basal motion. The 57
 nature of the hydrological system also plays a funda- 59
 mental role. These models specifically include a treat- 59
 ment of the basal hydrology, and its influence on basal 61
 movement (however caused), and allow fast ice flow 61
 only when the bed is melting and sub-glacial water 63
 pressures are high. Fowler and co-workers find that a 63
 'hydraulic runaway' exists in these models. Basal sliding 65
 is initiated when the bed reaches the melting point, and 65
 increases frictional heating of the bed. This increases 67
 water discharge, which for the hydrological configura- 67
 tion they envisage, leads to an increase in water 69
 pressure, and hence to an increase in sliding velocity, 69
 and higher frictional heating. This cycle is broken when 71
 the bed eventually re-freezes as a result of rapid thinning 71
 of the ice. The models used in these studies are zero- or 73
 one-dimensional, and cannot predict the spatial mani- 73
 festation of such surges. However, Fowler and co- 75
 workers suggest that for unconfined, two-dimensional 75
 flow, the instability may manifest itself as spatially 77
 discrete areas of fast flow, rather than as temporal 77
 switching (Fowler and Johnson, 1995; Fowler and 79
 Schiavi, 1998).
- Fowler's models assume some form of 'soft' bed 81
 condition, with basal motion controlled by sediment 81
 deformation. For these conditions, basal water pressure 83
 increases with water discharge, regardless of whether the 83
 water flows in a patchy film at the ice/bed interface 85
 (Alley, 1989), or in 'canals' incised into the till surface 85
 (Walder and Fowler, 1994). Such conditions are 87
 probably found beneath the present-day West Antarctic 87
 ice streams (Engelhardt and Kamb, 1997), although 89
 even in these conditions, there is evidence that basal 89
 sliding (or deformation of a very thin layer at the ice/till 91
 interface, rather than pervasive till deformation) ac- 91
 counts for the bulk of ice stream velocity (Engelhardt 93
 and Kamb, 1998). These 'soft' bed conditions may also 93
 have occurred in some areas overlain by Quaternary ice 95
 sheets at or near their maximum extent. However, they 95
 probably did not occur beneath the interior regions of 97
 such ice sheets, where the beds are generally of exposed 97
 bedrock, with a thin, discontinuous till cover. Never- 99
 theless, these areas show geomorphic evidence for fast 99
 ice flow (as discussed above). They are also charac- 101
 terised by the presence of eskers, which suggests that the 101
 hydrological configuration beneath these areas may 103
 have been very different (Clark and Walder, 1992). This 103
 is significant because, under steady state conditions at 105
 least, tunnel-based drainage systems are associated with 105
 an inverse relationship between water pressure and 107
 discharge (Röthlisberger, 1972).
- A separate problem here is the possible role played by 109
 the drainage of subglacial water in groundwater 109
 aquifers. In a series of one-dimensional model-based 111
 studies of groundwater flow, Boulton and co-workers 111
 (Boulton et al., 1995; Boulton and Caban, 1995) have

1 argued that for marginal areas of the Scandinavian ice
 3 sheet, underlain by Mesozoic and Cenozoic sedimentary
 5 rocks, the permeability of these beds is sufficient to drain
 7 meltwater beneath the ice sheet without the need for a
 9 hydrological system at the ice/bed interface. Thus,
 11 effective pressures in their model are high, suggesting
 13 basal hydrology has limited impact on ice dynamics
 15 (although ice dynamics are not explicitly modelled in
 17 their studies). This is seemingly contrary to most
 19 geological evidence, however, so they suggest that
 21 drainage through an overlying clay stratum (ignored in
 23 their studies) could produce a large drop in hydraulic
 25 potential across it, allowing low enough effective
 27 pressures at the upper surface of the layer to permit
 29 shear deformation. On the central shield areas of
 31 Scandinavia, however, bedrock permeabilities are insuf-
 33 ficient to drain meltwater, implying some form of
 35 hydrological system must occur at the ice-bed interface.
 37 The presence of eskers in these areas would seem to
 39 support this conclusion, and imply that the nature of the
 41 subglacial drainage system could affect ice sheet
 43 dynamics.

45 Boulton and co-workers assume that only water
 47 produced by basal melting will be present at the ice-
 49 bed interface. As discussed below, however, in this study
 51 we investigate the effects of allowing surface meltwater
 53 to reach the bed in certain circumstances. Surface
 55 melting is typically one to four orders of magnitude
 larger than basal melting (e.g. Boulton et al., 1995), and
 if such melt did reach the bed, it might supply sufficient
 water to require drainage at the ice-bed interface, even
 on the Mesozoic and Cenozoic aquifers. This would
 seem to provide an alternative solution to the problem
 of high effective pressures in these marginal areas in the
 reconstructions by Boulton et al. (1995) and Boulton
 and Caban (1995), as the basal hydrological system itself
 would determine effective pressure, rather than the
 transmissibility of the underlying aquifers.

Model-based studies of the Scandinavian ice sheet
 have adopted a variety of solutions to the problem of the
 apparent flow variability within this ice sheet. Early
 studies, in common with most ice sheet models, ignored
 the problem, leading to similar reconstructions to the
 CLIMAP study (Denton and Hughes, 1981), with large,
 thick, and quite static ice sheets. Other models have
 sought to allow fast sliding in particular areas of the ice
 sheet, and then examine its impact. These areas have
 often been chosen on the basis of geological evidence,
 and then imposed in the ice sheet model as a different
 basal boundary condition (e.g. Holmlund and Fastook,
 1993). Whilst this may allow the impact of particular
 areas of fast flow on the ice sheet dynamics to be
 evaluated, it does not allow the apparent variability of
 fast flow to be simulated, and nor does it address the
 question of why fast flow develops in particular areas,
 and not others, in the first place. A recent study by

Payne and Baldwin (1999) acknowledges these pro-
 blems, but adopts a different approach. They use a
 three-dimensional thermo-mechanical model, but ne-
 glect basal movement, instead concentrating on the
 strong dependence of ice viscosity on basal temperature,
 and the effect this has on ice dynamics under a steady
 climate. This paper does not attempt to produce a
 ‘geologically realistic’ reconstruction; rather, it seeks to
 explore the dynamic behaviour of an appropriately sized
 model ice sheet on a realistic topography, under certain
 conditions. This model develops discrete areas of faster
 flow around the margins, which match well with
 geological evidence, and which occur due to the feed-
 back between basal temperature and deformation
 velocity; warmer ice leads to fast flow, which lowers
 ice surface elevation, leading to fast flow due to the
 concentration of ice discharge (and hence heat produc-
 tion) in the faster flowing areas.

In this paper, we adopt a similar philosophy to this
 latter study. We do not seek to develop a ‘realistic’
 model of the Scandinavian Ice Sheet, but rather we
 focus on the potential impact of basal hydrology on ice
 sheet dynamics, through the possible feedbacks between
 the resulting ice sheet topography, flow and hydrology.
 We apply the model, with variable climate and mass
 balance parameters adjusted to give a realistically sized
 ice sheet at the LGM, on a realistic topography, using
 the Late Weichselian Scandinavian ice sheet as an
 example. The model presented here follows those of
 Fowler and co-workers by treating a melting bed as
 only a necessary condition for fast flow; low effective
 pressure must also be present if fast flow is to occur.
 The basal hydrological system is therefore modelled
 directly, and allowed to exist in either of two
 possible states; a ‘distributed’, cavity-based system,
 in which water pressure changes directly with
 water discharge (Kamb, 1987; Fowler, 1987a), or a
 tunnel-based system, with an inverse water pressure/
 discharge relationship. The transition between these
 two states is controlled using a stability criterion
 for tunnel-based flow (Fowler, 1987a, b). Basally
 produced meltwater and, under certain circumstances,
 surface meltwater supply the basal hydrological
 system. However, following the work of Payne and
 co-workers, the model has two spatial dimensions, and
 thus allows the impact of drainage system behaviour
 on the spatial and temporal variability of ice sheet
 flow to be evaluated. Our aim is to investigate
 how the dynamics of the model ice sheet are
 affected by the inclusion of a physically based
 model of sub-glacial hydrology. In particular, we are
 interested in whether the inclusion of such a model can
 lead to the degree of spatial and temporal flow
 variability that the geological record suggests, and
 which has generally not been captured by ice sheet
 models to date.

1 2. Model formulation

3 The model used in this study is a two-dimensional
 4 version of that used by Arnold and Sharp (1992) to
 5 investigate the influence of changing sub-glacial hydro-
 6 logy on the dynamics of the late Weichselian Scandina-
 7 vian ice sheet. Full details are given in the Appendix A,
 8 but we summarise the main features of the model here.
 9 It is based on a time-dependent mass continuity
 10 equation, solved using a semi-implicit, alternating
 11 direction, finite difference scheme. It simulates the
 12 time-dependent evolution of ice sheet form and flow.
 13 Ice is assumed to deform by simple shear, and sliding
 14 occurs where the base of the ice is calculated to be at the
 15 pressure melting point. A simple scheme, which com-
 16 pares heat produced at the base of the ice sheet (by
 17 geothermal and frictional heating) with the temperature
 18 gradient needed to conduct that heat away from the bed,
 19 is used to determine whether the glacier bed is at the
 20 pressure melting point (Arnold and Sharp, 1992). Any
 21 excess heat, which would raise the temperature above
 22 the pressure melting point, is assumed instead to melt
 23 basal ice. The resulting water then enters the modelled
 24 sub-glacial drainage system. This thermal scheme is very
 25 similar to that adopted by Fowler and co-workers
 26 (Fowler and Johnson, 1995, 1996; Fowler and Schiavi,
 27 1998), who assume that all heat produced by ice
 28 movement is produced in a boundary layer at the bed
 29 of the ice mass, in which the majority of shear occurs.
 30 This scheme therefore neglects the possible effects on
 31 basal temperatures of advection of cold ice from areas
 32 upstream or adjacent to areas in which fast flow occurs.
 33 However, in a two-dimensional flow-line study, Payne
 34 (1995) found that, even at some distance from the ice
 35 sheet margins, the advection of cold ice formed a minor
 36 component of the heat budget and had little effect on the
 37 basal temperature. This scheme also allows for effec-
 38 tively instantaneous transmission of surface temperature
 39 changes to the bed. Timescales of temperature diffusion
 40 in ice sheets can be approximated by dividing the ice
 41 thickness by the depth averaged vertical velocity, which
 42 can be taken to be half the accumulation rate (Paterson,
 43 1994, p. 338). At the divide at the LGM, modelled ice
 44 thicknesses are 2000–2500 m, and accumulation rates
 45 are $\sim 0.2\text{--}0.3\text{ m a}^{-1}$, giving a response time of 15,000–
 46 25,000 years. Nearer the ice sheet margins, or during
 47 deglaciation, thicknesses of $\sim 1000\text{ m}$ and accumulation
 48 rates of $\sim 0.5\text{ m a}^{-1}$ give response times of ~ 4000 years.
 49 We simulate this delay, and explore the model sensitivity
 50 to changing surface temperatures by ‘lagging’ the
 51 climatically induced surface temperature changes used
 52 in the calculations of basal temperature by a variable
 53 amount between 1000 and 20,000 years in some model
 54 runs.
 55 The sliding relationship used (McInnes and Budd,
 1984) depends on both the local shear stresses, and the

effective pressure (that is, the ice overburden pressure
 minus the subglacial water pressure). Since the effective
 pressure depends on the discharge in the sub-glacial
 drainage system, both the water inputs to this system,
 and the flow path followed by sub-glacial water must be
 known. There are two possible sources of water: basal
 melt and surface melt.

Evidence from esker sedimentology suggests that
 discharge in at least some sub-glacial tunnels varied on
 both diurnal (Allen, 1971) and annual (Banerjee and
 McDonald, 1975) time scales. Similarly, cyclic sequences
 in esker sediments have been linked to varved clays in
 pro-glacial lakes, which are demonstrably annual in
 origin (Kleman et al., 1997). This implies that surface-
 derived melt reached the ice sheet bed in some areas. For
 this to be possible, surface runoff must have penetrated
 significant thicknesses of ice at sub-freezing tempera-
 tures. Water draining into crevasses is a source of both
 sensible and frictional heat and, if discharge is sufficient,
 it may be capable of penetrating the subsurface cold
 layer and reaching ice at the pressure melting point
 below. Investigations of water flow, moulin water
 pressures, and glacier velocity on White Glacier, Axel
 Heiberg Island, suggest that surface streams with
 discharges of $0.1\text{--}0.2\text{ m}^3\text{ s}^{-1}$ could penetrate to the
 glacier bed through up to 300 m of cold ice (Iken,
 1974; Blatter, 1987). Another mechanism which might
 allow surface water to penetrate to the bed is the filling
 of surface crevasses by meltwater (Mavlyudov, 1995,
 1998; Scambos et al., 2000). Scambos et al., in a study of
 the breakup of Antarctic ice shelves, argue that melt-
 water can keep existing crevasses open in areas
 unfavourable to crevasse development, and that the
 pressure exerted by the water can lead to downwards
 propagation of the crevasse through the entire ice
 thickness if the crevasses are deeper than a critical
 depth (determined by factors including the fracture
 toughness of ice, ice density and the degree of water
 filling). Calculated critical depths are generally smaller
 than 20 m. Although this study is based on floating ice
 shelves, the key assumptions would seem applicable to
 ice sheets, especially in areas of longitudinal extension,
 as at the head of areas of fast ice flow in ice sheets.

To simulate these possibilities, we assume that surface
 melt can reach the bed if (a) the surface water discharge
 in a given grid cell exceeds some critical value (Q_{crit}), and
 (b) the base of the ice sheet in the grid cell is at the
 pressure melting point. We calculate the surface water
 discharge by integrating surface ablation rates down the
 ice sheet surface. In any cell with a bed temperature at
 the PMP, where the surface water discharge exceeds
 Q_{crit} , this discharge is added to any basal melt. To allow
 for the large thicknesses of cold ice which surface runoff
 must penetrate to reach the bed of ice sheets, we use
 $10\text{ m}^3\text{ s}^{-1}$ as an estimate of Q_{crit} in the ‘standard run’.
 The penetration of surface melt through ice sheets has

not been conclusively established, nor ruled out, so we investigate the impact of this assumption on basal hydrology and ice sheet flow dynamics by varying the value of Q_{crit} in a series of sensitivity analyses.

Once the quantities of basal melt, and surface melt which penetrate to the bed of the ice sheet, are known, these are integrated down the subglacial hydraulic potential surface (Shreve, 1972) to give the subglacial water discharge in each grid cell.

These calculations then allow the nature of the subglacial drainage system, and the resulting effective pressure to be calculated. Two possible configurations are allowed; a system of 'linked cavities' (Kamb, 1987), or a more efficient system of subglacial tunnels (Röthlisberger, 1972). Water pressures within these systems are calculated using the equations of Fowler (1987a, b). A stability criterion, following Fowler (1987a, b) is used to determine which type of drainage system dominates in each grid cell.

The model makes separate calculations of accumulation and ablation rates over the ice sheet. Precipitation rates across the study area at 120 ka BP were assumed to be the same as at the present day. This distribution was modelled using empirical relationships, which relate precipitation to latitude, longitude and elevation. During the model run, precipitation rates were altered as a function of the imposed temperature forcing and additional cooling associated with elevation changes induced by ice sheet growth and decay. These relationships do not account for possible changes of the atmospheric circulation that may have resulted from ice sheet growth and decay.

Ablation rates were calculated using the method of Budd and Smith (1981). The ablation rate is specified as a function of elevation relative to the elevation of the 1 m a^{-1} ablation contour (E_0), which is itself a function of latitude and the imposed temperature change, converted to an elevation change using a lapse rate of $6.5^\circ\text{C km}^{-1}$. Calving rates at marine margins of the ice sheet were determined using a water depth dependent calving law (Brown et al., 1982). These relationships all have obvious limitations. However, there are still enormous uncertainties about the climate during the Last Glacial period. We therefore justify the use of these relationships on the grounds that our aim is to investigate how the dynamics of the model ice sheet are affected by the inclusion of a physically based model of sub-glacial hydrology. We emphasise that we have not tried to produce as 'geologically realistic' a simulation of the ice sheet as possible.

Ice sheets exert a profound effect on bedrock topography through the process of isostasy. A variety of earth-models have been used in conjunction with ice sheet models to account for this effect (e.g. Le Meur and Huybrechts, 1996). However, many of the more physically realistic schemes have the disadvantage that

many parameter values needed are subject to a high degree of uncertainty. This can make within-model variations due to parameter uncertainties of the order of between-model variation due to model formulation (Le Meur and Huybrechts, 1996). Given these problems, and the aims of this study, we adopt a simple diffusion-based scheme to calculate the isostatic response to the growth and decay of the ice sheet.

3. Model inputs

The model requires two main input data sets; a Digital Elevation Model of the bedrock topography in the study area, and the forcing functions used to drive the model. The study area (Fig. 1) extends from approximately $50^\circ\text{N } 2^\circ\text{E}$ to $75^\circ\text{N } 50^\circ\text{E}$, and includes the whole of Scandinavia, the Baltic States and European Russia as far east as the Urals. The model uses a 40 km grid, which produced a 75 by 75 point DEM, using a Lambert conformal conic projection. At the start of a run (120 ka BP) the area is assumed to be ice free, and bedrock topography is assumed to be in isostatic equilibrium.

Forcing functions used to drive the model are eustatic sea level, taken from Shackleton (1987), and climatic change. The Laurentide ice sheet makes by far the largest contribution to eustatic sea level change, with the Scandinavian ice sheet responsible for perhaps 15–18 m out of a total change of c. 120 m at the LGM (Lambeck et al., 1998). We therefore treat eustatic sea level as an

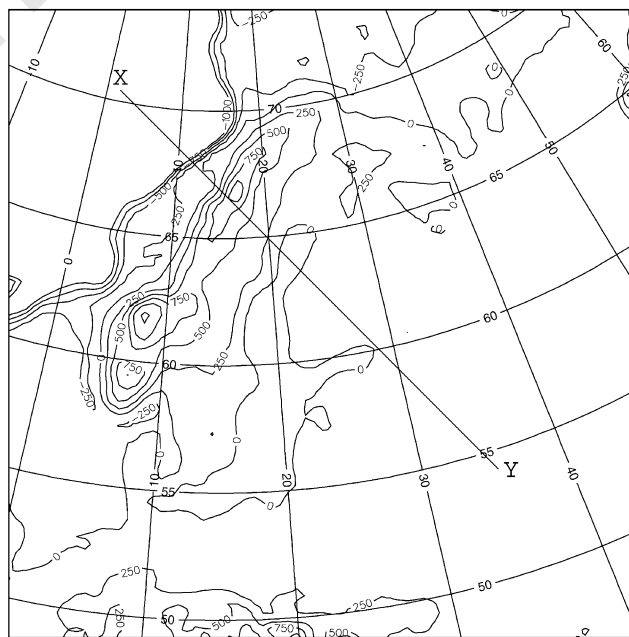


Fig. 1. Bedrock topography of the study area. Contours in m above sea level.

external variable. The GRIP $\delta^{18}\text{O}$ record (Johnsen et al., 1992; Dansgaard et al., 1993) was converted into an inferred temperature history using the conversion factor of $0.62 \delta^{18}\text{O K}^{-1}$ (Dansgaard et al., 1973) and used as the climatic forcing for the model. Although this is a very simple system, we justify it given our aims, which are to investigate the role of basal hydrology on ice sheet dynamics.

4. Results of the standard model

For these runs, the model is run from 120 ka BP to the present day. However, we focus the discussion on the Late Weichselian period, as geological evidence for the behaviour of the ice sheet is most plentiful for this time, and the larger ice sheet makes the impact of the changing ice sheet hydrology on the ice sheet behaviour more obvious. In the following discussion, the reference to periods and localities is for descriptive purposes only; we make no claims that the model is accurately predicting the occurrence of fast flow in particular times or places. We compare the behaviour of the model ice sheet with geological evidence in only in a qualitative sense. We are interested in whether the dynamic behaviour of the model and the nature of the hydrological system predicted are comparable with those inferred from geological evidence, rather than in exact spatial and temporal matches between the model and geological reconstructions.

As the model ice sheet grows towards its maximum extent, it develops unusual surface forms (Fig. 2), with distinct areas of the ice sheet showing convex-out lower elevation contours, but concave-out mid-elevation contours, which we call ‘lobes’. Such a lobe is always present over parts of southern Norway and Sweden (Location A in Fig. 2), in the south-western part of the ice sheet, but patterns of lobe development along the southern and eastern margins of the ice sheet vary over time. At 22,000 model years BP (Fig. 2a), there is a lobe over the Baltic Sea (Location B). At 18,000 model years BP (Fig. 2b), however, lobate areas occur on the eastern margins of the ice sheet over Finland and the Baltic States (Location C), rather than over the Baltic Sea. The lobes have narrow heads and became wider downstream. This configuration is similar to that of the lobes in the geologically based reconstructions of Punkari (1984), and to the ‘surge fans’ described by Kleman et al. (1997), although the model lobes can become very broad.

Throughout the period 22,000 model years BP to 18,000 model years BP, the ice divide shows a strong eastward convexity, caused by strong west or north-west ice flow over the lowest part of the Scandinavian mountain chain in central Norway, in broad agreement with Kleman et al. (1997). During ice sheet growth, the

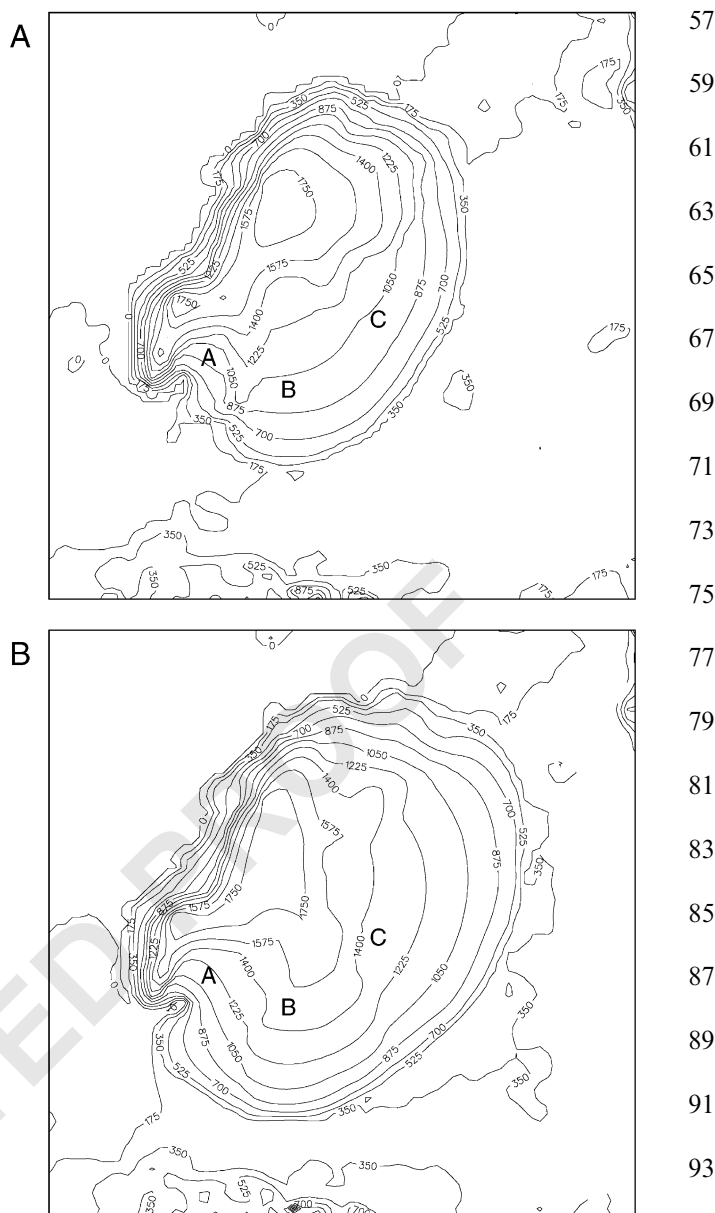


Fig. 2. Ice sheet (and surrounding topography) surface elevation. (a): At 22,000 yrs BP; (b): at 18,000 yrs BP. Contours in metres above contemporaneous sea level. For locations see text. X–Y denotes transect used in Figs. 7 and 9.

ice divide does not migrate very far to the east. It reaches the present-day western shore of the Gulf of Bothnia or a little further east between around 22,000 model years BP and 16,000 model years BP, before retreating west. During this period, however, the exact divide location fluctuates in response to lobe development. Dome surface elevations are quite low, with a maximum of around 2000m. The lobate flow pattern is clearly reflected in the ice sheet velocity field (Fig. 3a and b). Fast ice flow occurs throughout the period shown in Figs. 2 and 3 in the south west of the ice sheet (around the southern Norwegian/Swedish border, location A),

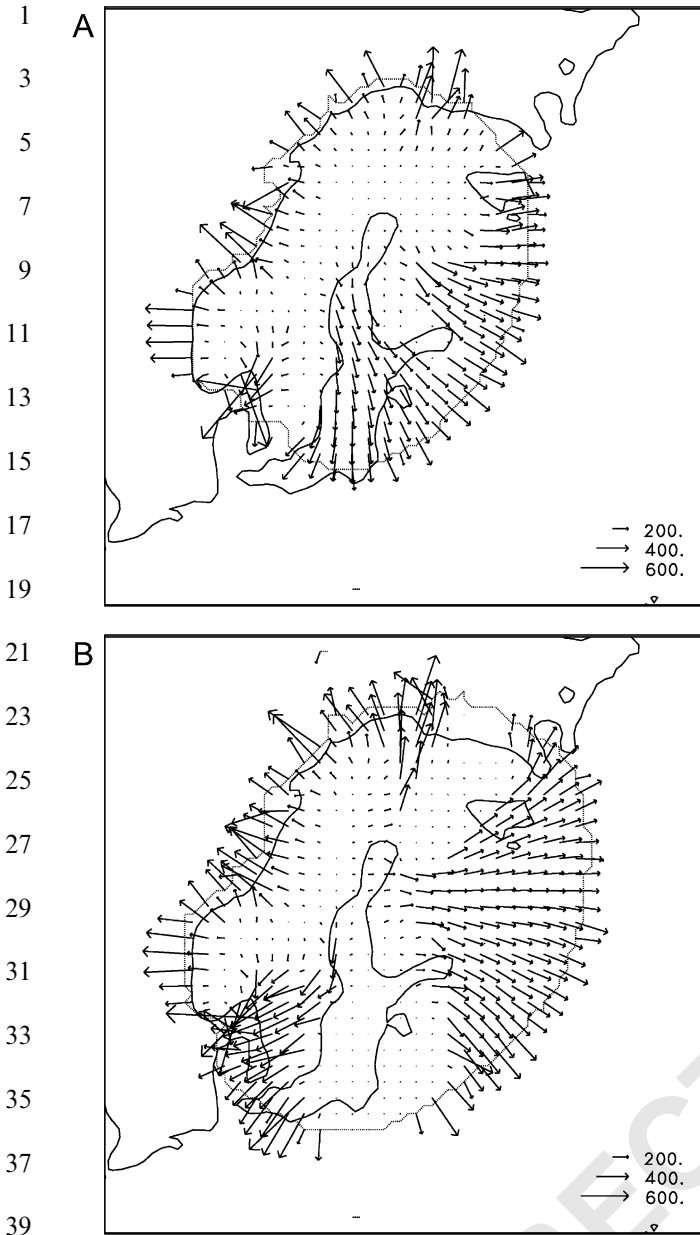


Fig. 3. Ice sheet velocity distribution. (a): At 22,000 yrs BP; (b): at 18,000 yrs BP. Values in m yr^{-1} .

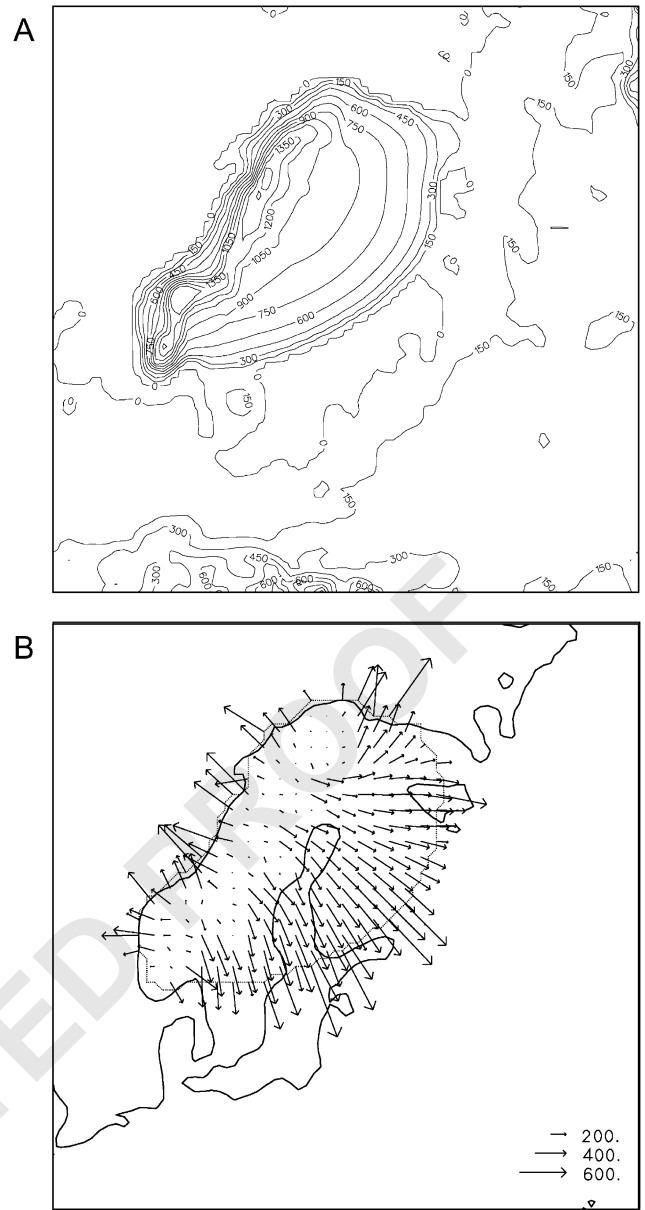


Fig. 4. Ice sheet configuration at 12,000 yrs BP. (a): Surface elevation, including surrounding topography (contours in metres); (b): velocity distribution (values in m yr^{-1}).

while changing patterns of fast flow occur on the southern (location B) and eastern margins (location C). Here, the areas of high velocity are associated with low surface slopes ($\sim 0.002\text{--}0.001$, c.f. slopes for Siple Coast ice streams of ~ 0.001 (Bentley, 1987)), while along the Norwegian margin of the ice sheet, and in the south west, high velocities occur in areas with steep surface slopes ($\sim 0.005\text{--}0.01$, c.f. slopes for Lambert Glacier of ~ 0.0075 (Bentley, 1987)).

After reaching its maximum areal extent at 16,300 model years BP (rather later than in many geological reconstructions), the ice sheet retreats rapidly. Fast ice flow transports large volumes of ice from the interior of

the ice sheet to the ablating margins and lowers the elevation of the ice sheet surface. At 12,000 model years, BP (the equivalent of the Younger Dryas Stade), the topographic effect of the lobes has become less obvious, but the velocity field shows three to five distinct lobes along the eastern margin, with differing flow directions and source areas (Fig. 4). This pattern of flow is in close agreement with the reconstructed ‘surge fans’ for this period in this region proposed by Kleman et al. (1997).

Cold-based ice occurs in central regions of the model ice sheet, with warm-based ice in marginal areas. In the model, the cold-based area is quite extensive during glacial build-up, and at the maximum extent (Fig. 5a).

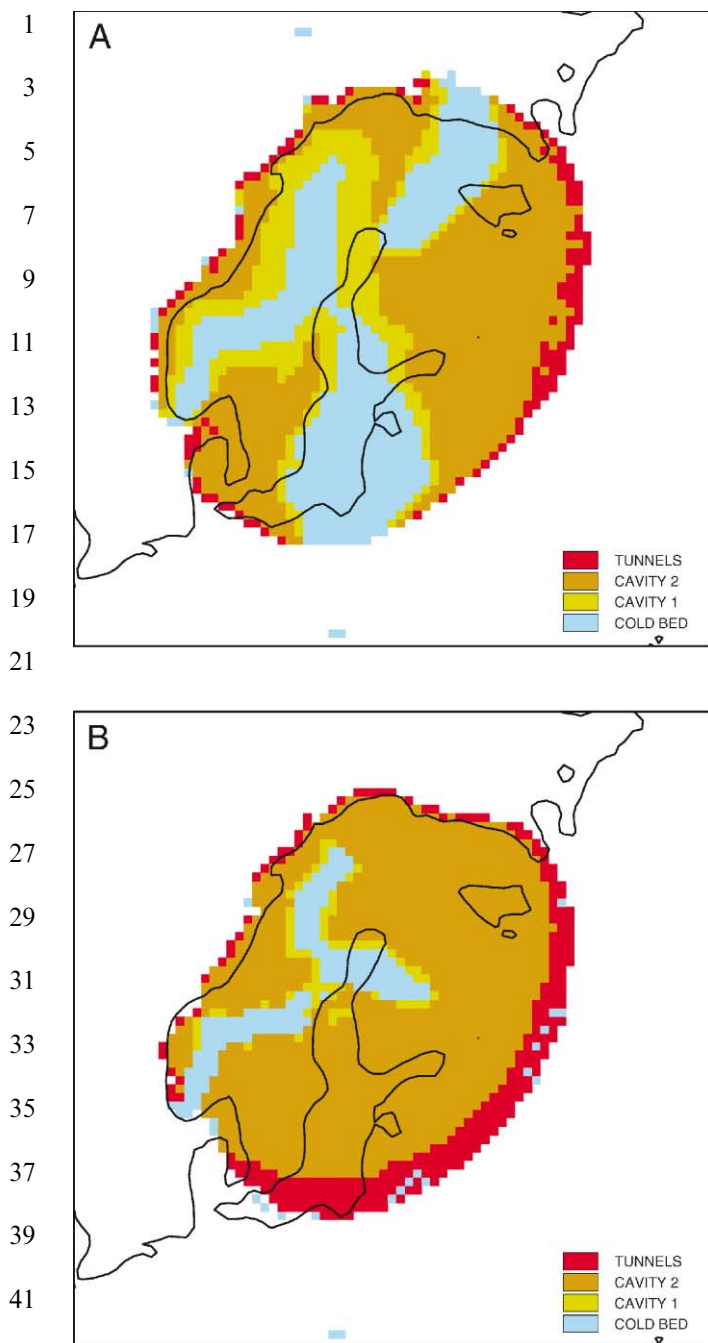


Fig. 5. Ice sheet basal conditions at (a): 18,000 yrs BP; (b): 14,000 yrs BP. Key: cold bed = ice below PMP; cavity 1 = ice at pressure melting point (PMP) but no surface water input, cavity-based drainage; cavity 2 = ice at PMP, surface water input, cavity-based drainage; tunnels = as cavity 2, but tunnel-based drainage.

Throughout the period, almost all of the central area beneath the divide remains frozen, but frozen areas near the margins are more variable, due to the growth and decay of the fast-flowing ice lobes discussed above. This frozen core gets disrupted, but never entirely disappears, during the rapid model deglaciation (Fig. 5b). This is in

close agreement with Kleman et al. (1997), who argue that the extensive preservation of landforms older than the LGM in central Scandinavia must imply a frozen bed. They also argue against massive binge-purge cycles (MacAyeal, 1993), affecting large areas of the ice sheet, but favour a stable, frozen core, with an intermediate zone with a 'fractal patchwork' (Kleman et al., 1997, p. 296) of frozen and thawed bed, and an outer wet-bed zone. This again is in qualitative agreement with the model results, which suggest that the development of wet-based, fast flowing lobes during ice sheet growth was spatially and temporally variable. We expect that such a pattern would leave a very complex landscape showing preservation of old features, areas of cross-cutting landforms, and areas typified by complete erosion of previous flow traces occurring in close proximity.

Within the warm based areas of the model ice sheet, basal water drainage is predominantly via linked-cavity systems, although tunnel-based drainage became established around the ice sheet margins during periods of warming climate. This is true during the growth phase, but especially during deglaciation (Fig. 5b), and particularly the final deglaciation after 16,000 yr BP, when increased meltwater fluxes lower sub-glacial water pressures. The warming climate means that large areas of the ice sheet experience surface melt, leading to high water inputs to the basal hydrological system. At this time, tunnels extend up to 160 km from the margin, though lengths of around 80 km are more normal. Typical discharges in sub-glacial tunnels at the ice sheet margin are of the order of $500 \text{ m}^3 \text{ s}^{-1}$ during the early stages of deglaciation (Fig. 6a), when catchment areas are large, falling to around $200 \text{ m}^3 \text{ s}^{-1}$ at 12,000 model years BP (Fig. 6b). These discharges are comparable to the value of $1000 \text{ m}^3 \text{ s}^{-1}$ used by Shreve (1985) for reconstructing ice sheet surface profiles from an esker system in Maine. To obtain such high discharge values, Shreve also assumed that surface melt reached the sub-glacial drainage system.

On account of the long water flow paths and low subglacial hydraulic potential gradients (due to the low ice surface and bed slopes), sub-glacial water pressures are typically 60–80% of ice overburden in tunnel-based systems and 85–95% of ice overburden in linked-cavity systems. Thus, the effect of changes in drainage configuration on ice sheet dynamics is relatively small, as high basal velocities occur even with tunnel-based drainage. This result is obviously dependent on the form of the sliding relationship used, and the parameter values chosen. However, the formation of fast-flowing lobes does not result from switching of the hydrological regime, but from the concentration of water flow into particular areas. This was controlled by the topographic evolution of the ice sheet and was affected only indirectly by the chosen sliding relationship.

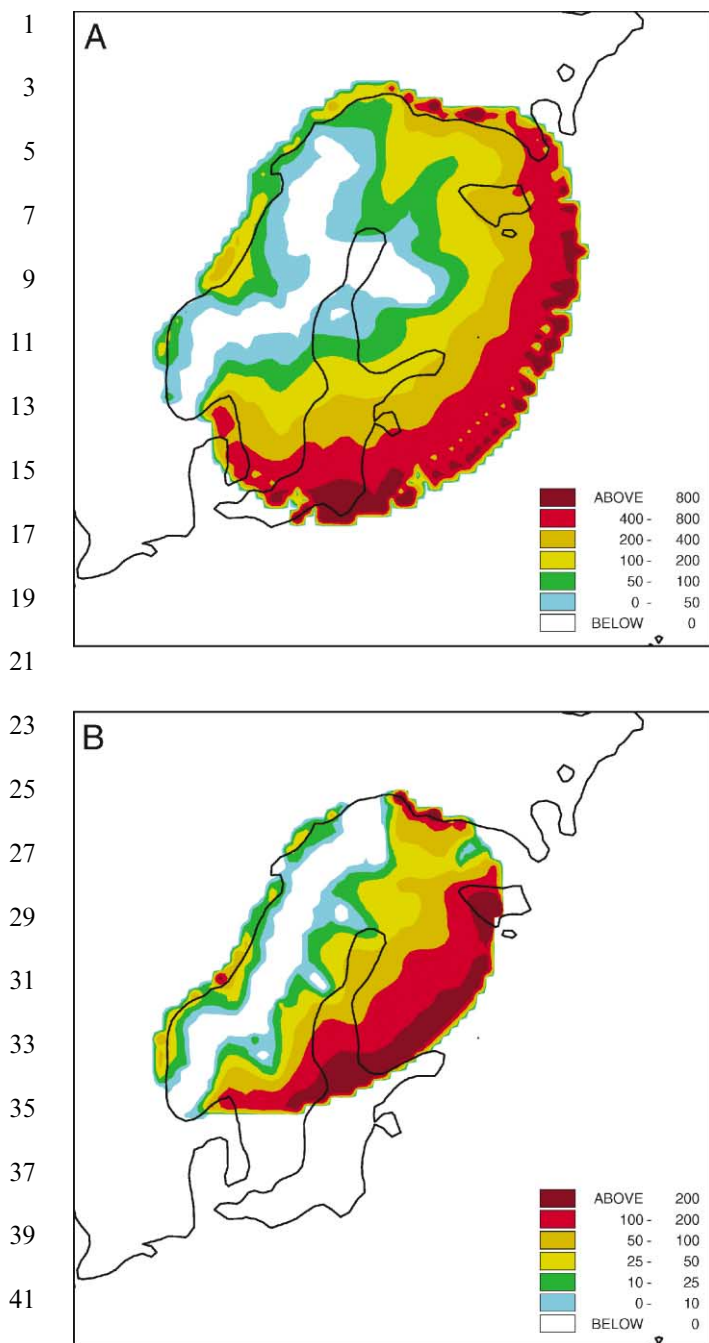


Fig. 6. Subglacial water discharge. (a): At 14,000 yrs BP; (b): At 12,000 yrs BP. Units are $\text{m}^3 \text{s}^{-1}$.

5. Model sensitivity to changes in the treatment of ice sheet hydrology

Given the aims of this study, we focus model sensitivity analysis on the hydrological model, rather than on the ice sheet model. There are two main aspects to this; the assumptions and parameter values adopted for the nature of the bed itself, such as tunnel and cavity spacing, bed roughness etc., and the influence of surface-

derived meltwater on processes at the bed. This also relates to the thermodynamic scheme adopted here, which does not allow for the advection of cold ice from upstream areas of the ice sheet, and assumes instantaneous transfer of surface temperature changes to the bed. We investigate this by conducting some simple experiments to investigate the control exerted by surface temperature changes on the basal temperature, by lagging the surface temperature changes used as input to the thermodynamic model, to simulate delayed response at the bed.

The earlier, one-dimensional version of the model (Arnold and Sharp, 1992) showed that the main impact of altering the hydrological system parameter values was on the nature of the hydrological system, rather than on the qualitative behaviour of the ice sheet as a whole. Experiments with the two-dimensional model not presented here also showed this. Assuming a smoother bed generally allowed tunnel-based drainage systems to be more common (and vice versa). Through changes in sub-glacial water pressure and hence ice velocity, this altered the exact spatial and temporal distribution of fast flowing lobes, but not their presence or absence. This implies that the development of a lobe at a particular time and place depends on the complex interplay of local ice and bed topography, water availability, and the bed configuration, and would thus be almost impossible to 'predict' in an exact sense.

In this paper we focus more on the role played by the amount of surface water at the bed, through the assumed critical discharge, and the role of basal temperature changes. Altering the degree to which surface melt could reach the bed had a much more profound effect on ice sheet development. Fig. 7 shows time-space diagrams of the extent of fast flow, and its temporal variability, for the period from 30,000 to 10,000 BP, for the NW–SE cross-section through the ice sheet shown in Fig. 1. A range of values of Q_{crit} from 2.5 to $50 \text{ m}^3 \text{ s}^{-1}$ was used, and a run was also performed in which no surface water is allowed to penetrate to the bed (effectively, an infinite Q_{crit}). This period is chosen as the ice sheet is largest, and so the effects are most apparent. In general, fast flow occurs more frequently as the ice sheet approaches its maximum extent, and during deglaciation. This is broadly climatic, as the warming climate means more meltwater is available. During growth, however, fast flow occurs intermittently, and the nature of the occurrence depends on the value of Q_{crit} . For very low values of Q_{crit} (below c. $5 \text{ m}^3 \text{ s}^{-1}$) (Fig. 7a), fast flow areas occur on the transect for more of the time, and some episodes last longer than others, although there is little apparent regularity. For Q_{crit} values $5\text{--}15 \text{ m}^3 \text{ s}^{-1}$ (Fig. 7b–e), the episodes of fast flow become more regular in extent and duration; they also tend to last longer, but happen less frequently as Q_{crit} increases. As Q_{crit} increases still further, and when no

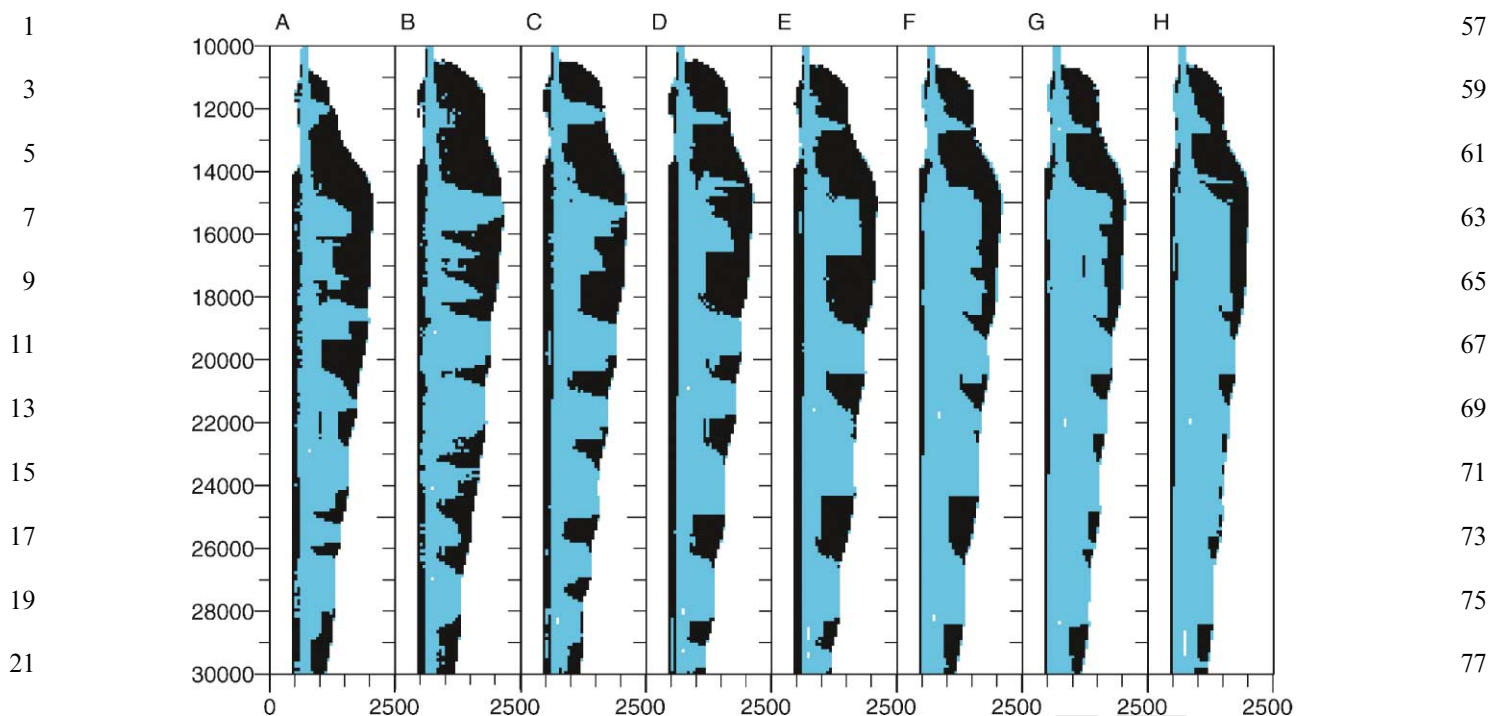


Fig. 7. Time-space diagrams of ice extent, and extent of fast flow from 30,000 yrs BP to 10,000 yrs BP, for transect X–Y in Fig. 1, with variable Q_{crit} values. X-axis units are km; black areas denote fast flow, blue areas denote slow flow. Fast flow is defined as areas of bed at the PMP, and with velocities in excess of 100 m a^{-1} . $A = Q_{crit}$ of $2.5 \text{ m}^3 \text{ s}^{-1}$; $B = Q_{crit}$ of $5 \text{ m}^3 \text{ s}^{-1}$; $C = Q_{crit}$ of $7.5 \text{ m}^3 \text{ s}^{-1}$; $D = Q_{crit}$ of $10 \text{ m}^3 \text{ s}^{-1}$; $E = Q_{crit}$ of $15 \text{ m}^3 \text{ s}^{-1}$; $F = Q_{crit}$ of $20 \text{ m}^3 \text{ s}^{-1}$; $G = Q_{crit}$ of $50 \text{ m}^3 \text{ s}^{-1}$; $H = \text{infinite } Q_{crit}$ (i.e. no surface water penetration).

surface water can reach the bed (Fig. 7f–h), fast flow becomes much more limited. Only as the ice reaches its maximum extent, and during deglaciation, does it play a significant role.

The spatial pattern of velocity is also affected by the value of Q_{crit} . For lower values a much smoother radial velocity pattern results, with no sharply defined, topographically lower, faster flowing areas (Fig. 8a, for a Q_{crit} of $2.5 \text{ m}^3 \text{ s}^{-1}$). In these cases, the fast flowing areas seem to cycle on and off across large areas of the ice sheet at once, in a manner analogous to the simple model of ‘binge-purge cycles’ developed by MacAyeal (1993), although with no obvious periodicity, as discussed above. For Q_{crit} values between around 5 and $15 \text{ m}^3 \text{ s}^{-1}$, the fast-flowing areas are generally lobate in form, similar to those produced in the ‘standard’ run. At high Q_{crit} values, the basal hydrology is again much more uniform spatially, with lower water discharges (and consequent lower water pressures in predominantly cavity-based drainage). Spatially patterns of ice flow are more uniform (Fig. 8b, for Q_{crit} of $50 \text{ m}^3 \text{ s}^{-1}$), driven by the much more uniform pattern of basal melting. This pattern also results if surface melt is not allowed to reach the bed.

Fig. 9 shows time-space diagrams for the runs in which surface temperature changes were lagged for the same time period and transect as Fig. 7. These show

some differences between the runs in terms of the exact spatial and temporal pattern of fast flowing areas, but the key qualitative aspects of model behaviour are preserved. No systematic trend in behaviour can be seen, suggesting that basal temperature, whilst affecting the detailed pattern of fast flow, does not play a primary role in controlling its development. The general correspondence in time for the occurrence of fast flow suggests that surface meltwater changes play a larger role than basal temperature changes, although it should be born in mind that the diagram only shows a one-dimensional transect through the ice sheet; fast flow may be occurring in adjacent areas of the ice sheet at times when the transect shown is flowing slowly, due to the spatial variability of fast flow in the model.

6. Discussion

The complex spatial and temporal evolution of the areas of fast flow, particularly during ice sheet growth, demands further explanation. Two aspects of the evolving flow pattern need to be considered: (i) how the lobate nature of the flow becomes established, and (ii) why the extent and location of areas of fast flow varies over time. In addition, this section considers the

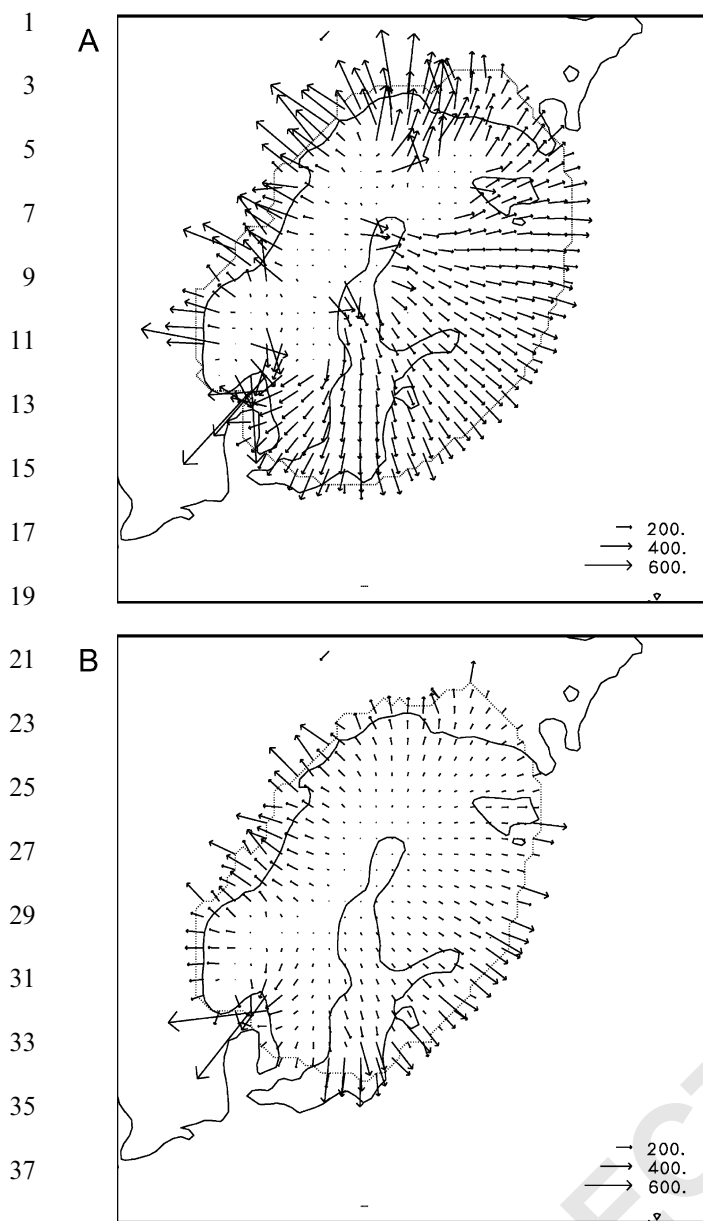


Fig. 8. Ice sheet velocity distributions at 18,000 yrs BP for different values of Q_{crit} . (a): $2.5 \text{ m}^3 \text{ s}^{-1}$; (b): $50 \text{ m}^3 \text{ s}^{-1}$.

impact of fast flow on the overall configuration of the ice sheet.

Due to the combination of high heat production (due to steep surface slopes) and high meltwater availability in marginal areas (within approximately 2–4 grid cells (80–160 km)) of the ice sheet, fast flow initially becomes established in these areas. At the upstream end of areas of fast flow, a ‘nick-point’ develops in the ice sheet surface. Here, the production of basal heat increases due to the combination of locally steeper surface slope and increasing basal velocity, and this allows head-ward expansion of the areas of fast flow. As this occurs at different rates in different parts of the ice sheet, both

surface and basal water flow become concentrated into areas of fast flow, which have the lowest surface elevations. This tends to result in further increases in basal velocity and frictional heating which favour continued head-wards expansion of the fast flowing areas into adjacent areas. The lowering of the surface also increases melting, and hence water discharge. This can result in an up-glacier expansion in the area of bed receiving surface melt, a further feedback effect. The spatial concentration of water flow into areas of thinner ice, or topographically lower areas, seems to prevent the whole of the ice sheet margin from experiencing fast ice flow. Flow concentration takes place both at the upstream areas of the lobes and at the lobe margins, where both surface and basal water flow are deflected towards the lobe, rather than towards the ice sheet margin. Bedrock topography plays a role in some areas, especially on the western side of the ice sheet, where topographic variation is strong and topographically controlled fast-flowing areas are relatively constant through time. On the eastern side, where the topography is much flatter, the evolving patterns of ice thickness (which dominate the basal hydraulic potential) are far more important.

The importance for lobe development of this mechanism of water flow concentration by ice sheet topography is underlined by the results of experiments in which the critical discharge value (Q_{crit}) for penetration of surface water to the bed was varied. Allowing surface water to penetrate at smaller discharges (and hence over larger areas) means that flow concentration does not occur. Large areas of the bed begin to receive surface melt, and so flow faster. This thins the ice, ultimately allowing the bed to re-freeze, leading to large-scale ‘binge-purge’ cycles affecting large areas of the ice sheet. For higher values of Q_{crit} , however, the process of lobe formation discussed above can begin to operate. In this case, individual areas of the ice sheet cycle between fast flow and slow flow, but as a viewed as a whole, the ice sheet is nearly always affected somewhere by fast flow, and so at a larger scale is more stable. As Q_{crit} increases further (or surface water is prevented from penetrating) the potential for flow concentration is reduced, as surface melt only reaches the bed very near the margins. Areas of fast flow are supplied mainly by basal melt, which is much more uniformly distributed spatially.

Several mechanisms combine to restrict the growth of areas of fast flow. As the areas of fast flow expand head-ward, they enter areas of the ice sheet with lower ablation rates. As a result, water flux through the fast flowing areas increases more slowly as these areas grow. This reduces the ‘per cell’ discharge, especially in upstream areas of the lobes, as the area experiencing fast flow increases more rapidly than water availability. Episodes of climatic cooling also reduce meltwater availability. Both of these effects reduce sliding and

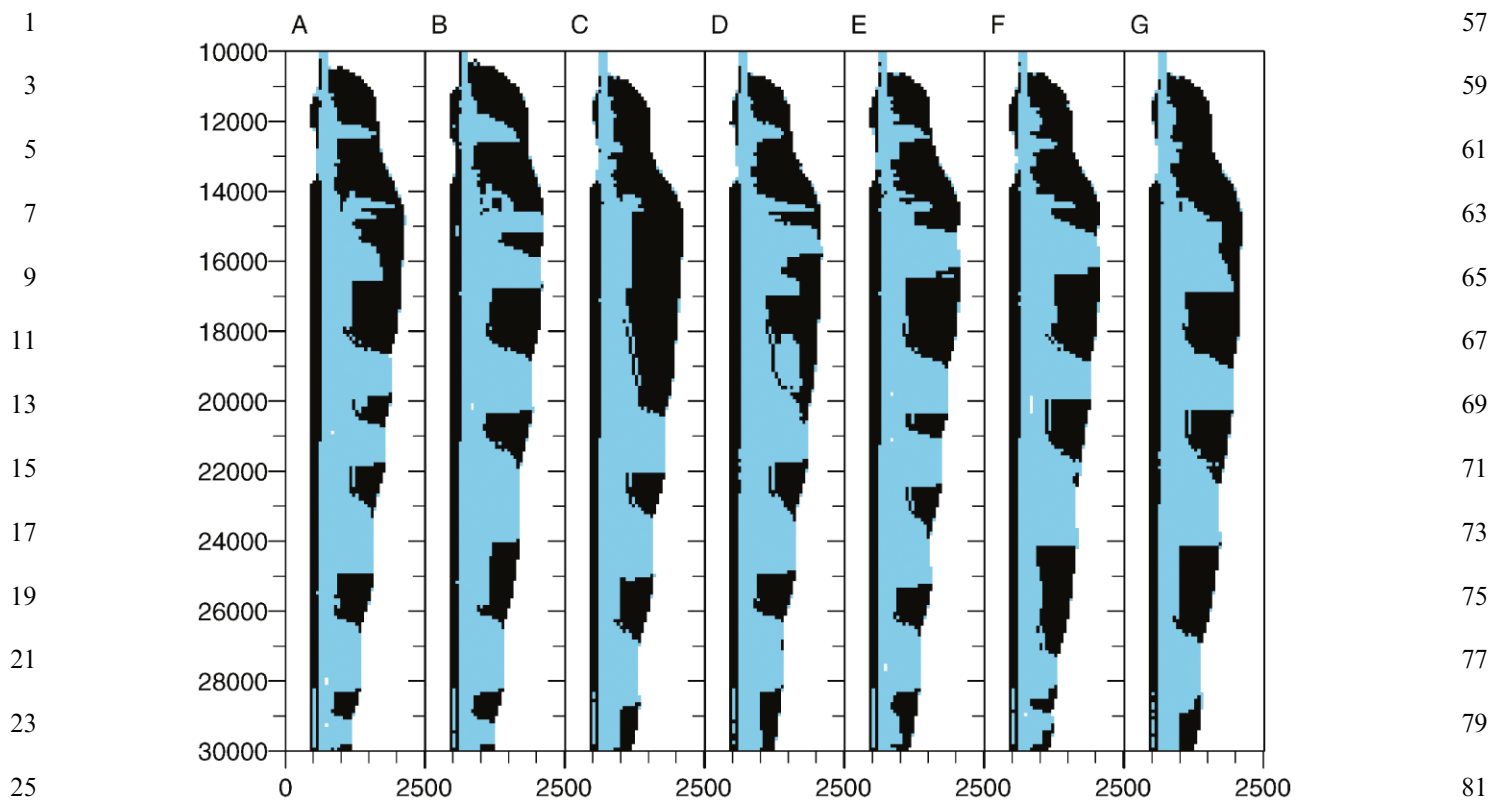


Fig. 9. Time-space diagrams of ice extent, and extent of fast flow from 30,000 yrs BP to 10,000 yrs BP, for transect X–Y in Fig. 1, with lagged surface temperature inputs for basal temperature calculations. X-axis units are km; black areas denote fast flow, blue areas denote slow flow. Fast flow is defined as areas of bed at the PMP, and with velocities in excess of 100 m a^{-1} . Lag times: *A* = 0 years (i.e. standard run); *B* = 1000 years; *C* = 2000 years; *D* = 5000 years; *E* = 10,000 years; *F* = 15,000 years; *G* = 20,000 years.

frictional heating (due to the fall in water pressure in cavity-based drainage as water discharge falls), which reduces ice sheet velocity and allows the ice sheet bed to re-freeze. These factors seem to have a much larger, and more immediate impact, than the change in basal temperature due to climate, as shown by the small changes in the qualitative model behaviour where surface temperature changes are lagged at the bed. This perhaps suggests that fracture-induced penetration of surface meltwater to the ice sheet bed is a mechanism by which surface temperature changes might be transmitted very rapidly to the bed. Refreezing of such water at the cold bed would supply latent heat, which together with viscous dissipation, could warm the bed rapidly, allowing sliding and the consequent increase in frictional heating, further aiding the development of fast flow. The basal temperature thus depends very much on changes in local heat production induced by hydrological changes. As velocities fall, surface elevation tends to increase, further reducing ablation rates, concentration of meltwater flow, downstream water flux and the extent of areas of water-lubricated fast sliding. In large lobes, the establishment of tunnel-based drainage near the ice sheet margin results in a small further decrease in water pressure, and hence sliding velocity in such areas. This

leads to upstream thickening of the ice, and hence lower water production, which also restricts the headwards growth of the lobes.

Furthermore, as the areas of fast flow expand headwards into the ice sheet interior, their upper areas start to interact, and ‘capture’ water from each other. This diversion of water flow rapidly reduces sub-glacial water discharge in the ‘captured’ lobe. As a result, sliding velocities fall, reducing basal friction and allowing the bed temperature to drop below the melting point. This is illustrated in Fig. 4, which shows how by 18 ka BP the small lobes which existed over Finland (area C) and southern Norway (area A) at 22 ka BP (Fig. 4a) have expanded headwards into the ice sheet (Fig. 4b), capturing water which previously flowed beneath the ‘Baltic Sea’ (area B) ice lobe. As a result, this lobe has ceased to exist.

These processes are therefore controlled more by the local variation in basal heat production itself, rather than by the loss of heat to the ice sheet surface. Thus, the rapid switch-off of fast flowing areas would seem quite realistic; the reduction in heat production due to the thinner ice and lower ice velocity as water pressures drop would be felt very rapidly at the bed, independently of the rate of heat loss due to thinning ice and/or

1 surface temperature changes being conducted to the bed.
 2 This again would seem to be born out by the
 3 insensitivity of the model to ‘lagged’ surface temperature
 4 changes.

5 A fundamental problem therefore seems to be what
 6 mechanisms control the oscillation of the bed about the
 7 pressure melting point. The two possible controls would
 8 seem to be the climate changes at the surface, or the
 9 changes in ice sheet geometry and dynamics, and the
 10 resulting changes in basal heat production. The fact that
 11 lagging surface temperature changes at the bed makes
 12 little overall difference to the model results seems to
 13 suggest that the latter mechanism dominates, and that
 14 the impact of surface temperature changes on basal
 15 temperature is less important. However, the fact that
 16 fast flow does tend to occur at certain times more
 17 frequently than at others, and also occurs over a wider
 18 area of the ice sheet during warming episodes (especially
 19 the main deglaciation phase after ~18,000 BP) suggests
 20 that surface temperature changes can be important.
 21 Thus, some mechanism to allow the (near) instantane-
 22 ous transfer of surface temperature changes to the bed
 23 must also be required; the penetration of surface
 24 meltwater to the bed, possibly by fracture propagation,
 25 would seem to provide this. The role of surface
 26 temperature variations on changing in basal tempera-
 27 ture would seem to be further complicated by the fact
 28 that during the last 20,000–30,000 years of a glacial
 29 cycle, a series of temperature perturbations driven by
 30 Dansgaard–Oerscher events will be arriving at the bed.
 31 This may well affect the precise timing of basal warming
 32 and cooling in particular areas, but it would not seem to
 33 invalidate the major controls on basal conditions
 34 explored in this study, and their impact on ice sheet
 35 dynamics.

36 As discussed above, these changes in ice sheet
 37 hydrology and velocity seem to match qualitatively with
 38 geological reconstructions of the dynamics of the
 39 Scandinavian ice sheet. These have shown lobate
 40 patterns of flow in the central areas of Scandinavia,
 41 and also rather complex evolution of these patterns
 42 spatially and temporally (e.g. Kurimo, 1978; Punkari,
 43 1984; Kleman et al., 1997). The predicted mode of
 44 retreat of the ice sheet, in which an area of tunnel-based
 45 sub-glacial drainage near the ice sheet margin retreats
 46 up-glacier as the margin retreats, also matches well with
 47 geological evidence for esker formation and glacier
 48 dynamics in southern Sweden. This suggests that eskers
 49 were formed time-transgressively beneath a retreating
 50 ice sheet margin (Hebrand and Amark, 1989).

51 The relatively thin model ice sheet has a more linear
 52 surface profile on its eastern margin than in the west.
 53 This contrasts with the ice sheet morphology produced
 54 by models without basal slip, which show a parabolic
 55 profile with rapid thickening away from the margin. The
 linear surface profile is largely caused by the high ice

discharge from central areas into the ice lobes. The new
 reconstruction matches well with isostatically based
 reconstructions of the Scandinavian ice sheet (Lambeck
 et al., 1998). These suggest that, for plausible values of
 lithosphere thickness and mantle viscosity, maximum ice
 sheet thicknesses at the LGM are around 2000 m,
 located to the west of the Gulf of Bothnia, compared
 with the 3400 m thick ice sheet divide over the Gulf of
 Bothnia suggested by Denton and Hughes (1981). The
 thinner, isostatically derived ice sheet thicknesses are
 similar to those produced in the model discussed here,
 which suggests thicknesses of around 1800 m over the
 Gulf of Bothnia, and 2000 m at the divide, slightly to the
 west.

The results of this study, in which the ice sheet as a
 whole is affected by fast flow in some areas throughout
 growth and decay of the ice sheet, but particularly
 during deglaciation, also agree qualitatively with the
 reconstructions of Boulton et al. (2001). They argue that
 perennial streaming would be a mechanism to reconcile
 the apparent mismatch in ice thickness between most
 model-based reconstructions, and the isostatic evidence
 for ice thickness discussed above.

7. Conclusions

Inclusion of basal hydrology in a model of the
 Scandinavian Ice Sheet produces behaviour that seems
 to match qualitatively with that inferred from geological
 evidence. Spatially and temporally variable zones of fast
 flow develop within the ice sheet through mechanisms
 which are entirely internal to the model, and are not
 contingent upon the specification of locally distinct
 basal boundary conditions for their formation (c.f.
 Holmlund and Fastook, 1993). The presence of ex-
 tensive areas of fast flow results in a relatively thinner ice
 sheet, particularly in central and eastern Scandinavia.
 This matches well with isostatically based reconstruc-
 tions of ice sheet thickness. The variability of the warm-
 bedded fast-flowing areas in the standard run, located
 towards the margin from a frozen-bed ‘core’ area within
 the ice sheet also matches well with geological evidence,
 and seems to argue against massive binge-purge cycles
 affecting large areas of an ice sheet (Macayeal, 1993);
 rather, the flow variability is manifest at a more local
 scale within the ice sheet.

The mechanism by which fast flow occurs in the
 model involves the accentuation of the impact of initial
 changes in basal temperature by the concentration of
 meltwater flow into those areas where the basal ice
 reaches the pressure melting point. Flow concentration
 is linked to changes in ice sheet surface topography and
 their effect on the form of the sub-glacial hydraulic
 potential surface. The model also shows that discrete
 areas of fast flow develop when surface melt is input to

the bed of the ice sheet in particular areas. They do not develop when surface water inputs are absent or distributed across the entire ice sheet ablation area.

Concentration of meltwater flow, both on the surface of the ice sheet and at the bed (due to variations in the sub-glacial hydraulic potential), tends to increase sub-glacial water pressures (due to the distributed nature of the drainage system over much of the bed). Through the water-pressure dependent sliding law, this increases basal sliding and heat production. In turn, this causes further changes in ice sheet geometry and patterns of surface and basal water flow and results in headwards growth of areas of fast flow. This positive feedback cycle is halted by a series of factors that eventually limit the availability of water at the base of the ice sheet. The formation of discrete areas of fast flowing ice, separated by slower ice, has been observed in other ice sheet models. It is due to interactions between ice flow, basal temperature and basal sliding (e.g. Payne and Dongelmans, 1997; Payne et al., 2000), or to interactions between ice temperature and rates of ice deformation (e.g. Payne and Baldwin, 1999). Thus, the spatial differentiation of flow produced in this study is not unique. What seems to be new to this model, however, is the temporal variability of flow within the lobes. This has been observed in a two-dimensional flowline ice sheet model (e.g. Payne, 1995). However, it does not generally occur in map-plane models (either two-dimensional or three-dimensional), in which the ice lobes seem to be more permanent features (e.g. Payne and Dongelmans, 1997; Payne and Baldwin, 1999; Payne et al., 2000). The exception to this is the study by Payne (1998), in which the Siple Coast area of West Antarctica does show temporal flow variability, as fast flowing areas seem to ‘capture’ ice from each other. In the current study, however, the variations in hydrology driven by the impact of topographic changes acting internally to the model allow fast flowing areas to switch on and off. This is due to processes occurring within the lobes themselves, as well as to interactions between the lobes through a *water capture* mechanism. Climatic changes can also lead to hydrological changes (due to varying water discharges, and hence water pressure) and can act as an external forcing mechanism, increasing flow variability.

The model does not include the effect of advection of cold ice from upstream (or laterally from inter-lobate areas). If included in the model, this might also slow the head-ward penetration of the zones of fast flow into the ice sheet interior. However, it is unlikely that this would preclude the basic mechanism by which changes in ice sheet topography lead to concentration of water flow into particular areas of the ice sheet. Neither would it preclude the possibility that these areas interact to cause switches in the flow regime in other parts of the ice sheet. Nevertheless, work is underway to include the physically

based treatment of basal hydrology developed here in a full thermo-mechanically coupled ice sheet model to address this issue.

Acknowledgements

This work was undertaken while NA held a UK Natural Environment Research Council Studentship at Cambridge University, and the manuscript was begun while NA held an Isaak Walton Killam Memorial Post-doctoral Fellowship at the University of British Columbia. We also thank the referees, Richard Hindmarsh, Neil Humphrey, Garry Clarke and Tony Payne for their helpful comments on the manuscript.

Appendix A. Model formulation

The ice dynamics model used here is a conventional, two-dimensional planar model for ice flow. All parameter values are given in Table 1. It uses the continuity equation to calculate the evolution of ice thickness through time

$$\frac{\partial Z}{\partial t} = A_c - A_b - \nabla(\bar{U}Z), \quad (\text{A.1})$$

where Z is the ice thickness, ∇ the two-dimensional horizontal divergence operator, A_c the local accumulation rate, A_b the local ablation rate and \bar{U} the vertically integrated two-dimensional horizontal velocity, resulting from deformation of the ice, and in certain circumstances, sliding of the ice over its bed. This is solved using a semi-implicit, alternating direction implicit finite difference scheme, following Press et al. (1992).

Ice deformation is assumed to be driven solely by the horizontal basal shear stresses (τ_b), which are approximated by

$$\tau_{bx} = \rho_i g Z \frac{\partial E}{\partial x} \quad (\text{A.2})$$

in the x direction, where E is the ice surface elevation, g is gravity, and ρ_i is ice density, and similar for the y direction.

The resulting vertically integrated ice deformation velocity is then calculated from Glen’s flow law

$$U_{dx} = \frac{2A}{n+2} \tau_b^{n-1} \tau_{bx} Z, \quad (\text{A.3})$$

where U_{dx} is the x component of the deformation velocity, A is the temperature dependent Arrhenius relation, and n is usually taken to be 3. τ_b is derived from the two-dimensional surface slope, in an equivalent equation to A2. This relationship assumes that ice deformation is laminar, and occurs under simple shear, and is unaffected by longitudinal stresses.

1 Table 1
Model parameter values

3 *Ice flow*

5 Deformation
Multiplier A 5.3×10^{-15} $s^{-1} k Pa^{-3}$
Power n 3.0 —

7 Sliding
1st multiplier K_1 6.3×10^{-5} $m^2 s^{-1} k Pa^{-1}$
2nd multiplier K_2 400 M

11 Drainage configuration
Latent heat L 3.3×105 $J kg^{-1}$
Channel flow f 700 $m^{-8/3} kg$
13 No. of cavities N_K 30000 —
Cavity X-section S_K 10^{-2} m^2
15 Shadowing function S 0.5 —
Bedrock amplitude a 1 m
17 Bedrock wavelength l 5 m
Ratio a/l v 0.2 —
Power function m 2.0 —

19 Ice conductivity K 2.1 $J s^{-1} m^{-1} K^{-1}$
21 Ice density ρ_i 900 $kg m^{-3}$
Water density ρ_w 1025 $kg m^{-3}$
23 Gravity G 9.81 $m s^{-2}$

Isostasy
25 Mantle density ρ_m 3300 $kg m^{-3}$
Mantle diffusivity Da 1.11 $m^2 s^{-1}$

27 *Precipitation parameterisation*
29 c_1 0.8 $m a^{-1}$
 c_2 0.004 $m a^{-1} \Psi^{-}$
 c_3 0.003 $m a^{-1} \phi^{-}$
31 — 25000 —
 c_5 2500 m
33 c_6 10 $m \Psi^{-1}$
 c_7 25 $m \phi^{-}$
35 c_8 0.85 —
 c_9 1000 —

37 Sliding velocity also depends to some extent on the
41 local basal shear stress, but is also assumed to be water
43 pressure dependent. We use the sliding 'law' of McInnes
and Budd (1984)

45
$$U_{SX} = k_1 \tau_{bX} / (N + k_2 N^2), \quad (A.4)$$

47 where U_{sx} is the x component of the sliding velocity, N
is the calculated effective pressure (that is, the ice
49 overburden pressure minus the subglacial water pres-
sure), and k_1 and k_2 are empirical parameters.

51 Sliding only occurs if the bed is at the pressure melting
53 point, and we use a simple scheme to calculate the basal
55 temperature, based on the heat supplied to the bed by
geothermal heating and friction from ice movement, and
the temperature gradient needed to conduct that heat
away. The frictional heat supplied to the bed (H) is

calculated from

57
$$H = \rho_i \frac{dE}{dx} Q_i, \quad (A.5) \quad 59$$

where Q_i is the ice discharge. It can be assumed that this
61 heating occurs only at the bed, and so this, together with
the geothermal heat flux (G) can then be compared with
63 the temperature gradient needed to conduct the heat
65 away

67
$$H + G = K \frac{\partial T}{\partial z}, \quad (A.6) \quad 67$$

where $\partial T / \partial z$ is the vertical temperature gradient and K
69 the thermal conductivity of ice. If the surface tempera-
71 ture is known, the basal temperature can be calculated
from

73
$$T_b = T_s + ZH/K, \quad (A.7) \quad 73$$

where T_b is the basal temperature, and T_s the surface
75 temperature. Any excess heat is used to melt basal ice. T_s
is calculated from the climatic forcing, the ice sheet
77 elevation, and the equilibrium line altitude, assuming a
79 temperature at the equilibrium line of $-15^\circ C$ (Oerle-
mans, 1982).

The model calculates the effective pressure using the
81 equations of Fowler (1987a). The effective pressure
varies depending on whether the basal drainage system
83 consists of large, widely spaced, efficient conduits or
tunnels, or an inefficient system of linked cavities.

For tunnels, effective pressure is calculated as

85
$$N_R = [(\rho_w g \phi Q_R) / (\rho_i A F S_K)]^{1/n}, \quad (A.8) \quad 87$$

where N_R is the effective pressure for a tunnel based
89 system, ρ_w the water density, g the acceleration due to
gravity, Q_R the volume flux of meltwater, ρ_i the ice
91 density, A the Arrhenius parameter, F the latent heat, n
the exponent in Glen's flow law, S_R the tunnel cross
93 sectional area, and ϕ is the hydraulic gradient, defined as

95
$$\phi = \alpha + [(\rho_w - \rho_i) / \rho_w] \beta. \quad (A.9) \quad 95$$

Here β is the bed slope. S_R is calculated as

97
$$S_R = (f Q_R^2 / \rho_w g \phi)^{3/8}, \quad (A.10) \quad 99$$

where f is an empirical constant related to turbulent
99 channel flow.

For cavities, effective pressure is calculated as

101
$$N_K = r [(\rho_w g \phi) / (\rho_i A F) (Q_K n_K S_K)]^{1/n}, \quad (A.11) \quad 103$$

where N_K is effective pressure for a cavity based system,
105 r is a shadowing function (Liboutry, 1978), defined as
the probability that a randomly selected area of the bed
is in contact with the ice, $Q_K = Q_R$ the volume flux of
107 meltwater, n_K is the number of passageways across the
width of the glacier and S_K is the cross-sectional area of
109 a typical passageway.

Following Fowler (1987a), a stability criterion for
111 tunnel flow is used to determine which type of system

1 exists in each grid cell at each time-step
 2 $A = vU_s/1AN^n$ (A.12)
 3

4 where $v = (a/l)$, a is typical bedrock bump amplitude, l
 5 is typical bump wavelength and A is the Arrhenius
 6 parameter.

7 The critical value for tunnel stability, A_c , is given by
 8 $A_c = (3nS_R/A^*)^{[(4-\mu)/\mu]}$ (A.13)
 9

10 where A^* is the total cavity cross sectional area, and μ
 11 the power function for self-similar bedrocks (Fowler,
 12 1987a, b).

13 This criterion assumes that a tunnel-based system can
 14 exist alongside a cavity-based system, which will drain
 15 areas of the bed between the tunnels. The stability
 16 criterion calculates the stability of the tunnel-based
 17 system in the presence of cavities, by comparing the
 18 relative changes in water pressure as discharge changes
 19 in the two systems. Tunnel-based systems are generally
 20 stable for situations with high water discharge, low
 21 water pressure and slow-moving ice. If tunnels are found
 22 to be stable, they are assumed to dominate the drainage
 23 system and to carry all of the sub-glacial water. Water
 24 pressure is calculated accordingly (Eq. (A.8)). If tunnels
 25 are unstable, the water is assumed to drain through a
 26 cavity-based system, and Eq. (A.11) for cavity-based
 27 drainage is used. Fowler's published values for the bed
 28 roughness parameters and cavity size and spacing are
 29 used throughout the model (Table 1). If tunnel-based
 30 drainage is predicted, it is assumed that there is one
 31 tunnel in each 40 km grid cell, consistent with the
 32 observed esker spacing of approximately 30 km in south-
 33 ern Finland (Geological Survey of Finland, 1984).

34 Eqs. (A.6) and (A.9) both require the subglacial
 35 discharge to be known. To calculate this, surface melt
 36 is routed across the ice sheet surface using an 'upstream
 37 contributing area' algorithm described by Sharp et al.
 38 (1993). Water discharge is integrated along each flow
 39 path until it exceeds the critical value, at which point it
 40 is added to the rate of basal melt in that cell. The same
 41 'upstream contributing area' algorithm is used to
 42 calculate basal discharge in each cell by integrating the
 43 combined surface and basal inputs down the sub-glacial
 44 hydraulic potential surface

45 $\Phi = \rho_w g B + \rho_i g Z,$ (A.14)

46 (Shreve, 1972) where B is the bedrock elevation, until
 47 the ice sheet margin is reached. This method assumes
 48 that meltwater generated in interior regions of an ice
 49 sheet can reach the margin in less than one model time
 50 step. For a 1500 km wide ice sheet and 10 year time step,
 51 this implies that water flows at $> 5 \times 10^{-3} \text{ m s}^{-1}$. Dye
 52 tracing results from modern glaciers generally yield flow
 53 velocities higher than this (e.g. Behrens et al., 1975;
 54 Fountain, 1993), although it is of similar magnitude to
 55 velocities in distributed systems.

The model makes separate calculations of accumula- 57
 tion and ablation rates over the ice sheet. Precipitation 59
 rates across the study area at 120 ka BP were assumed to 61
 be the same as at the present day. This distribution was 62
 modelled using empirical relationships, which relate 63
 precipitation to latitude, longitude and elevation. Dur- 64
 ing the model run, precipitation rates were altered as a 65
 function of the imposed temperature forcing and 66
 additional cooling associated with elevation changes 67
 induced by ice sheet growth and decay. These relation- 68
 ships to do not account for possible changes of the 69
 atmospheric circulation that may have resulted from ice 70
 sheet growth and decay. They assume that a 'sea-level 71
 equivalent' precipitation (P_0) value can be defined for 72
 north-west Europe, based largely on distance from the 73
 Atlantic Ocean (assumed to be the main water vapour 74
 source), latitude, and temperature. This precipitation 75
 value thus decreases towards the north and east

76 $P_0 = c_1 - c_2\psi - c_3\varphi - c_4\Delta E_0,$ (A.15) 77

78 where ψ is the longitude, φ the latitude, ΔE_0 the change 79
 in elevation of the 1 m a^{-1} ablation contour (see below), 80
 and c_1 to c_4 are adjustable parameters. 81

82 This calculated 'sea level' precipitation is then 83
 subjected to orographic enhancement, up to a critical 84
 height (E_m), at which moisture exhaustion is assumed 85
 to occur, and above which precipitation will start to 86
 decrease. This critical height again depends on latitude, 87
 longitude and temperature change

88 $E_m = c_5 - c_6\psi - c_7\varphi - c_8\Delta E_0,$ (A.16) 89

90 where c_5 to c_8 are again adjustable parameters. The 91
 precipitation value (P_m) at this altitude is then 92
 calculated from

93 $P_m = P_0(2^{E_m/c_9}),$ (A.17) 94

95 where c_9 is an adjustable parameter. From P_0 , P_m and 96
 E_m , a precipitation gradient with altitude is calculated 97
 (P_g), and the actual precipitation value (P) in a 98
 particular grid cell, at a particular surface elevation 99
 (E) is calculated from

100 $P = [P_0 + EP_g] - P_m(2^{(E-E_m)/c_9}) + [P_0 + EP_g]$ (A.18) 101

102 if $E < E_m$, and

103 $P = P_m/(2^{(E-E_m)/c_9})$ (A.19) 104

105 if $E \geq E_m$.

106 Values for c_1 to c_9 were derived by making an initial 107
 guess for their values, and then approximating optimal 108
 values by comparing the resulting predicted precipita- 109
 tion field by eye for western Europe with published 110
 precipitation maps (UNESCO, 1970). Accumulation 111
 rates (A_c) were calculated from predicted precipitation 112
 values using an empirical effectiveness relationship

1 (Payne, 1988)

$$3 \quad A_c = -0.698P + 0.014\phi + 0.224\Delta E_0. \quad (A.20)$$

5 Values of c_4 and c_8 , which control the response to
 7 climate change were adjusted by running the model with
 9 different values until predicted ice sheet extent approxi-
 11 mately matched that inferred from geological evidence.

13 Ablation rates were calculated using the method of
 15 Budd and Smith (1981).

$$11 \quad \log_{10} Ab = \frac{1}{\kappa}(E_0 - E), \quad (A.21)$$

13 where E_0 is the elevation of the 1 ma^{-1} ablation
 15 contour, which is itself a function of latitude and the
 17 imposed temperature change, converted to an elevation
 19 change using a standard lapse rate of $6.5^\circ\text{C km}^{-1}$.

21 Calving rates at marine margins of the ice sheet were
 23 determined using a water depth dependent calving law
 25 (Brown et al., 1982)

$$19 \quad V_c = 27.1W, \quad (A.22)$$

21 where V_c is a calving velocity, and W is the water depth
 23 at the ice margin. V_c is converted to a volume loss by
 25 multiplying by the ice thickness in a calving cell. This is
 27 incorporated into the continuity equation by adding any
 29 calving to the ablation rate. These relationships all have
 31 obvious limitations. However, there are still enormous
 33 uncertainties about the climate during the last glacial
 35 period. We therefore justify the use of these relation-
 37 ships on the grounds that our aim is to investigate how
 39 the dynamics of the model ice sheet are affected by the
 41 inclusion of a physically based model of sub-glacial
 43 hydrology. We emphasise that we have not tried to
 45 produce as 'geologically realistic' a simulation of the ice
 47 sheet as possible.

49 Isostatic response is calculated using a diffusion-based
 51 scheme

$$37 \quad \frac{\partial B}{\partial t} = \text{Da} \nabla^2 (B - B_0 + L), \quad (A.23)$$

39 where Da is mantle diffusivity, B_0 is the original
 41 unloaded topography, and L is the imposed load,
 43 defined as $Z\rho_i/\rho_m$, where ρ_m is the mantle density.

45 References

- 47 Allen, J.R.L., 1971. A theoretical and experimental study of climbing-
 49 ripple cross-lamination, with a field application to the Uppsala
 51 esker. *Geografiska Annaler* 53A, 157–187.
 53 Alley, R.B., 1989. Water pressure coupling of sliding and bed
 55 deformation: I. Water system. *Journal of Glaciology* 35, 108–118.
 Arnold, N., Sharp, M., 1992. Influence of glacier hydrology on the
 dynamics of a large quaternary ice sheet. *Journal of Quaternary
 Science* 7, 109–124.
 Banerjee, I., McDonald, B.C., 1975. Nature of esker sedimentation.
 In: Jopling, A.V., McDonald, B.C. (Eds.), *Glaciofluvial and
 glaciolacustrine sedimentation*. Society of Economic Palaeontolo-
 gists and Mineralogists, Special Publication 23, Tulsa, OK, pp.
 132–154.

- Behrens, H., Bergmann, H., Moser, H., Ambach, W., Jochum, O., 57
 1975. On the water channels of the Hintereisferner, Ötztal Alps,
 Austria. *Journal of Glaciology* 14, 375–382. 59
 Bentley, C.R., 1987. Antarctic ice streams: a review. *Journal of*
Geophysical Research 92 (B9), 8843–8858. 61
 Blatter, H., 1987. On the thermal regime of an Arctic valley glacier—a
 study of White Glacier, Axel-Heiberg island, NWT, Canada.
Journal of Glaciology 33, 200–211. 63
 Bond, G., Heinrich, H., Broecker, W., Labeyrie, L., McManus, J.,
 Andrews, J., Huon, S., Jantschik, R., Clasen, S., Simet, S.,
 Tedesco, K., Bonani, G., Ivy, S., 1992. Evidence for massive
 discharges of icebergs into the North Atlantic during the last glacial
 period. *Nature* 360, 245–249. 67
 Boulton, G.S., Caban, P., 1995. Groundwater flow beneath ice sheets:
 Part II—its impact on glacier tectonic structures and moraine
 formation. *Quaternary Science Reviews* 14, 563–587. 69
 Boulton, G.S., Caban, P., 1995a. Groundwater flow beneath ice sheets:
 Part I—Large scale patterns. *Quaternary Science Reviews* 14,
 545–562. 71
 Boulton, G.S., Clark, C.D., 1990b. A highly mobile Laurentide ice
 sheet revealed by satellite images of glacial lineations. *Nature* 346,
 813–817. 73
 Boulton, G.S., Clark, C.D., 1990. The Laurentide ice sheet through
 the last glacial cycle: the topology of drift lineations as a key to the
 synamic behaviour of former ice sheets. *Transactions of the Royal
 Society of Edinburgh, Series Earth Science* 81, 327–347. 77
 Boulton, G.S., Dongelmans, P., Punkari, M., Broadgate, M., 2001.
 Palaeoglaciology of an ice sheet through a glacial cycle: the
 European ice sheet through the Weichselian. *Quaternary Science
 Reviews* 20, 591–625. 79
 Boulton, G.S., Hindmarsh, R.C.A., 1987. Sediment deformation
 beneath glaciers: rheology and geological consequences. *Journal*
of Geophysical Research 92 (B9), 9059–9082. 83
 Brown, C.S., Meier, M.F., Post, A., 1982. Calving speed of Alaska
 tidewater glaciers, with application to Columbia Glacier. US
 Geological Survey Professional Paper 1258-C., 15pp. 87
 Budd, W.F., Smith, I.N., 1981. The growth and retreat of ice sheets in
 response to orbital radiation changes. Sea level, Ice and Climatic
 Change. Proceedings of the Canberra Symposium, December 1979.
 IAHS Publication no. 131, 369–409. 89
 Clark, C.D., 1993. Mega-scale glacial lineations and cross-cutting ice-
 flow landforms. *Earth Surface Processes and Landforms* 18, 1–29. 91
 Clark, P.U., Walder, J.S., 1992. Subglacial drainage and deforming
 beds beneath the Laurentide, British and Scandinavian ice sheets.
EOS, Transactions of the American Geophysical Union 73,
 159–160 (Abstract only). 95
 Dansgaard, W., Johnsen, S.J., Clausen, H.B., Gundestrup, N., 1973.
 Stable isotope glaciology. *Meddelelser om Grønland* 197, 53. 97
 Dansgaard, W., Johnsen, S.J., Clausen, H.B., Dahl-Jensen, D.,
 Gundestrup, N.S., Hammer, C.U., Hvidberg, C.S., Steffensen,
 J.P., Sveinbjörnsdottir, A.E., Jouzel, J., Bond, G., 1993. Evidence
 for general instability of past climate from a 250-kyr ice-core
 record. *Nature* 364, 218–220. 101
 Denton, G.H., Hughes, T.J., 1981. *The Last Great Ice Sheets*. Wiley,
 New York, 484pp. 103
 Dyke, A.S., Morris, T.F., 1988. Canadian landform examples 7.
 Drumlin fields, dispersal trains and ice streams in arctic Canada.
The Canadian Geographer 32, 86–90. 105
 Dyke, A.S., Prest, V.K., 1987. Last Wisconsinan and Holocene history
 of the Laurentide ice sheet. *Geographie et Physique Quatenaire* 41,
 237–264. 107
 Engelhardt, H., Kamb, B., 1997. Basal hydraulic system of a West
 Antarctic ice stream: constraints from borehole observations.
Journal of Glaciology 44, 223–230. 109
 Engelhardt, H., Kamb, B., 1998. Basal sliding of Ice Stream B, West
 Antarctica. *Journal of Glaciology* 44, 223–230. 111

- 1 Fountain, A.G., 1993. Geometry and flow conditions of subglacial
water at South cascade glacier, Washington state, USA; an analysis
of tracer injections. *Journal of Glaciology* 30, 180–187.
- 3 Fowler, A.C., 1987a. Sliding with cavity formation. *Journal of
Glaciology* 33, 255–267.
- 5 Fowler, A.C., 1987b. A theory of glacier surges. *Journal of
Geophysical Research* 92 (B9), 9111–9120.
- 7 Fowler, A.C., Johnson, C., 1995. Hydraulic runaway: a mechanism for
thermally regulated surges of ice sheets. *Journal of Glaciology* 41,
554–561.
- 9 Fowler, A.C., Johnson, C., 1996. Ice sheet surging and ice-stream
formation. *Annals of Glaciology* 23, 68–73.
- 11 Fowler, A.C., Schiavi, E., 1998. A theory of ice sheet surges. *Journal of
Glaciology* 44, 104–118.
- 13 Geological Survey of Finland, 1984. Quaternary Deposits of Finland.
1:1,000,000.
- 15 Hebrand, M., Åmark, M., 1989. Esker formation and glacier dynamics
in eastern skåne and adjacent areas, southern Sweden. *Boreas* 18,
67–81.
- 17 Holmlund, P., Fastook, J., 1993. Numerical modelling provides
evidence of a Baltic Ice Stream during the Younger Dryas. *Boreas*
22, 77–86.
- 19 Huybrechts, P., 1992. The Antarctic ice sheet and environmental
change: a three-dimensional modelling study. *Berichte zur Polar-
forschung* 99, 241.
- 21 Iken, A., 1974. Velocity fluctuations of an Arctic valley glacier, a study
of White Glacier, Axel Heiberg Island, Canadian arctic Archipe-
lago. Axel Heiberg Island Research Reports, McGill University,
Montreal, Canada, *Glaciology* No. 5, 116pp.
- 23 Iken, A., 1981. The effect of the subglacial water pressure on the sliding
velocity in an idealised numerical model. *Journal of Glaciology* 27,
407.
- 25 Iverson, N.R., Jansson, P., Hooke, R.L., 1995. Flow mechanism of
glaciers on soft beds. *Science* 267, 80–81.
- 29 Johnsen, S.J., Clausen, H.B., Dansgaard, W., Fuhrer, K., Gundestrup,
N., Hammer, C.U., Iversen, P., Jouzel, J., Stauffer, B., Steffensen,
J.P., 1992. Irregular glacial interstadials recorded in a new
Greenland ice core. *Nature* 359, 311–313.
- 31 Kamb, B., 1987. Glacier surge mechanism based on linked cavity
configuration of the basal water conduit system. *Journal of
Geophysical Research* 92 (B9), 9083–9100.
- 33 Kleman, J., Hättstrand, C., Borgström, I., Stroeven, A., 1997.
Fennoscandian palaeoglaciology reconstructed using a glacial
geological inversion model. *Journal of Glaciology* 43, 283–299.
- 35 Kurimo, H., 1978. Late-glacial ice flows in northern Kainuu and
Peräpohjola, north-east Finland. *Fennia* 156, 11–43.
- 37 Lambeck, K., Smither, S., Johnston, P., 1998. Sea-level change, glacial
rebound and mantle viscosity for Northern Europe. *Geophysical
Journal International* 134, 102–144.
- 39 Le Meur, E., Huybrechts, P., 1996. A comparison of different ways of
dealing with isostasy: examples of modelling the Antarctic ice sheet
during the last glacial cycle. *Annals of Glaciology* 23, 309–317.
- 41 Lindstrom, D.R., 1990. The Eurasian ice sheet formation and collapse
resulting from natural atmospheric CO₂ concentration variation.
Paleoceanography 5, 207–227.
- 43 MacAyeal, D.R., 1993. Binge/purge oscillations of the Laurentide ice
sheet as a cause of the North Atlantic's Heinrich events.
Paleoceanography 8, 775–784.
- 45 Mathews, W.H., 1974. Surface profiles of the Laurentide Ice Sheet in
its marginal areas. *Journal of Glaciology* 13, 37–43.
- Mavlyudov, B.R., 1995. Problems of en- and subglacial
drainage. *Annales littéraires de l'université de Besançon*, no.
561, série Géographie no. 34. Actes du troisième symposium
international Cavités glaciaires et cryokarst en régions polaires
et de haute montagne. Chamonix, France, September 1994,
pp. 77–82.
- Mavlyudov, B.R., 1998. Glacier caves origin. *Salzburger Geogra-
phische Materialien*. Vol. 28. Fourth international symposium on
glacier caves and cryokarst in polar and high mountain regions,
September 1996. Salzburg, Austria, pp. 123–130.
- McInnes, B.J., Budd, W.F., 1984. A cross-sectional model for West
Antarctica. *Annals of Glaciology* 5, 95–99.
- Paterson, W.S.B., 1994. *The Physics of Glaciers*, 3rd Edition.
Pergamon/Elsevier, Oxford.
- Payne, A.J., 1988. Modelling former ice sheets. Ph. D. Thesis,
Edinburgh University, Edinburgh, UK, 211pp.
- Payne, A.J., 1995. Limit cycles in the basal thermal regime of ice
sheets. *Journal of Geophysical Research* 100 (B3), 4249–4263.
- Payne, A.J., 1998. Dynamics of the Siple Coast ice streams, West
Antarctica: results from a thermomechanical ice sheet model.
Geophysical Research Letters 25, 3173–3176.
- Payne, A.J., 1999. A thermomechanical model of ice flow in West
Antarctica. *Climate Dynamics* 15, 115–125.
- Payne, A.J., Dongelmans, P.W., 1997. Self-organisation in the
thermomechanical flow of ice sheets. *Journal of Geophysical
Research* 102 (B6), 12219–12233.
- Payne, A.J., Huybrechts, P., Abe-Ouchi, A., Calov, R., Fastook, J.L.,
Greve, R., Marshall, S.J., Marsiat, I., Ritz, C., Tarasov, L.,
Thomassen, M.P.A., 2000. Results from the EISMINT model
intercomparison: the effects of thermomechanical coupling. *Journal
of Glaciology* 46, 227–239.
- Punkari, M., 1984. The relations between glacial dynamics and tills in
the eastern part of the Baltic Shield. In: Königsson, L.-K. (Ed.),
Ten Years of Nordic Till Research, Vol. 20. Striae, pp. 49–54.
- Punkari, M., 1989. Glacial dynamics and related erosion-deposition
processes in the Scandinavian ice sheet in south-western Finland: a
remote sensing, fieldwork and computer modelling study. Helsinki,
Academy of Finland. Research Council for the Natural Sciences.
Final Report, Project 01/663. 86pp.
- Röthlisberger, H., 1972. Water pressure in intra- and subglacial
channels. *Journal of Glaciology* 11, 177–203.
- Scambos, T.A., Hulbe, C., Fahnestock, M., Bohlander, J., 2000. The
link between climate warming and break-up of ice shelves in the
Antarctic Peninsula. *Journal of Glaciology* 46, 516–530.
- Shackleton, N.J., 1987. Oxygen isotopes, ice volume and sea level.
Quaternary Science Reviews 6, 183–190.
- Sharp, M., Richards, K.S., Arnold, N.S., Lawson, W., Willis, I.,
Nienow, P., Tison, J.-L., 1993. Geometry, bed topography and
drainage system structure of the Haut Glacier d'Arolla, Switzer-
land. *Earth Surface Processes and Landforms* 18, 557–571.
- Shreve, R.L., 1972. Movement of water in glaciers. *Journal of
Glaciology* 11, 205–214.
- Shreve, R.L., 1985. Late Wisconsin ice surface profile calculated from
esker paths and types, Katahdin Esker System, Maine. *Quaternary
Research* 23, 27–37.
- UNESCO, 1970. *Climate Atlas of Europe*.
- Walder, J.S., Fowler, A.C., 1994. Channelized subglacial drainage over
a deformable bed. *Journal of Glaciology* 40, 3–15.